Steady-Wave Analysis of the Effect of Porosity on Viscous and Inviscid Detonations by Use of a Reactive-Porous Analog

LOS ALAMOS SCIENTIFIC LABORATORY
Post Office Box 1663 Los Alamos, New Mexico 87545

UNITED STATES
DEPARTMENT OF ENERGY
CONTRACT W-7405-ENG. 36

LA-7819
UC-34
Issued: September 1979

Steady-Wave Analysis of the Effect of Porosity on Viscous and Inviscid Detonations by Use of a Reactive-Porous Analog

R. L. Rabie

STEADY-WAVE ANALYSIS OF THE EFFECT OF POROSITY ON VISCOUS AND INVISCID DETONATIONS BY USE OF A REACTIVE-POROUS ANALOG

by

R. L. Rabie

ABSTRACT

A simple two-rate reactive material analog is used to determine reactive flow in a slightly porous medium. The rates govern the evolution of a chemical reaction coordinate and a solid volume coordinate, respectively. The rates are coupled so that "mechanical" phenomena can affect "chemical" phenomena and vice versa. Steady waves in both viscous and inviscid flow have been examined, with variations in ignition criteria being of prime interest in the viscous flow. A particular result is that the steady-state detonation velocity depends upon the ignition conditions.

I. INTRODUCTION

In shock-compression of solids one tends to associate porosity with dissipation of energy. This dissipation near a particular pore or void is an irreversible process that generates internal entropy, which causes localized heating. The material is assumed to respond to this preferential heating in some characteristic manner. If the material is an explosive one generally expects enhanced reaction at these local "hot spots."

The theorists' problem is to specify this irreversible process of pore crush-up in terms of bulk material properties and to combine this process with other pertinent rate functions, in particular the chemical rates.

In an experiment, the problem is somewhat different in setting, although the solution must agree with the correct theoretical prediction. An apparently comprehensive one-dimensional experiment involves acquisition and direct Lagrangian analysis of stress-time records at several material positions in a given sample.[1] This analysis provides a history of the specific internal energy, stress, particle velocity, and density at each material point covered by the gauge data. When an equation of state is given, one can solve for the reaction coordinate λ at each material point in the experimental range. These data are compared with predictions, and the theory is adjusted to lead to agreement.

Complications arise when the experiment involves an additional rate, and thus an additional progress variable ν. Unless λ or ν is measured independently, direct analysis will give only a relation of the form

$$\lambda = \lambda(\nu)$$

at each point in the reaction zone, and even that changes from point to point. Thus one is generally not able to separate out the varying effects of the two different rates. One might ask whether any useful information may be obtained from direct analysis at all concerning the individual rates. The development of a simple two-rate material analog is begun here with the ultimate intent being a test of direct analysis.

This report examines theoretically the steady-flow behavior of a simple reactive porous material. Steady waves are assumed and their profiles are obtained in both inviscid and viscous flow. The effects of varying elementary material parameters, such as the viscosity coefficient, the "q" of reaction, rate multipliers, and ignition conditions, are examined with respect to changes in the steady-wave profiles. Inviscid flow is examined first to define the terminology and to orient the reader to the problem.

The first four sections are given to the inviscid problem. The second of these deals with the chemical and mechanical rates. The third discusses the equation of state and the fourth the steady-frame equations. The fifth section combines the first three and sets forth the problem to be solved and its solution in considerable detail. Section six sets forth the viscous flow equations in the steady frame together with a restatement of the rates and equation of state. The viscous problem is stated and its solution is presented. Also presented is a detailed study of variations in the viscous problem allowed by the introduction of viscosity. A particular example is variation in ignition conditions. The final section, seven, is given to discussion and conclusions. The outline of a followup report on time-dependent calculations is also contained in this section.

II. CHEMICAL AND MECHANICAL RATES

The two rate laws given govern the evolution of the mass fraction of reacted material denoted by λ, and the evolution of the solid volume fraction ν. The ratio ν of the specific bulk density to the matrix or solid density is evaluated at some point in the material. The physical limits on ν are $0 \leq \nu \leq 1$, in which $\nu = 0$ implies no solid volume, i.e., all void, and $\nu = 1$ implies no voids. The limits on λ are conventional with $0 \leq \lambda \leq 1$, and $\lambda = 1$ is totally reacted. I will call the λ rate a chemical rate and the ν rate a mechanical rate. The chemical rate is

$$\left(\frac{\partial \lambda}{\partial t}\right)_x + u \left(\frac{\partial \lambda}{\partial x}\right)_t = \dot{\lambda} = \left(\frac{k_1}{\rho}\right) (1-\lambda)^2 \nu \quad . \tag{1}$$

The mechanical rate is

$$\left(\frac{\partial \nu}{\partial t}\right)_x + u \left(\frac{\partial \nu}{\partial x}\right)_t = \dot{\nu} = \left(\frac{k_2}{\rho}\right) (1-\lambda)(1-\nu) \quad . \tag{2}$$

The additional parameters are rate multipliers k_1 and k_2; new variables are position x, time t, x-frame particle velocity u, and density ρ.

The first thing to note about Eqs. (1) and (2) is that the chemical and mechanical rates are coupled. By doing this I have in mind the following picture of this material; since pore crush-up leads to the formation of centers of concentrated energy I would like to enhance the chemical rate in some manner related to pore crush-up.[2] This is done by the addition of the factor ν in the chemical rate. Thus, as $\nu \to 1$ from its initial value, say 0.9, the chemical rate is slightly increased. Additionally, as chemical reaction proceeds and some voids are filled with reacted products I would like the mechanical rate to be decreased in agreement with the thought that a void filled with reacted products is no longer discernible as a void.[2] Thus the factor $(1 - \lambda)$ is used in the mechanical rate to accomplish this. The occurrence of $(1 - \lambda)^2$ in the chemical rate is simply a mathematical convenience as is the presence of the density. This will become clear when the steady-frame equations are set forth in Sec. IV.

The rates displayed in Eqs. (1) and (2) are set to zero in the initial state and, in the inviscid case, are to be turned on at the arrival of the detonation wave. This "shock jump" ignition necessitated by the lack of viscosity is remedied in Sec. VI.[3]

III. THE EQUATION OF STATE

The material equation of state that gives the material's response to equilibrium processes is

$$p = \frac{1}{2} a^{\circ}(\rho - \rho_o)^2 + \lambda q_1 + (1 - A\lambda)(\nu - \nu_o)\, q_2 \quad . \tag{3}$$

The parameters are ρ_o - the initial density, a° - a constant of magnitude 1 carrying units of [pressure/(density)^2], q_1 - a constant pressure of chemical reaction, q_2 - a constant pressure of mechanical reaction, A - a constant whose value (between 1 and 0) allows zero, partial, or complete memory of the pressure of mechanical reaction, and ν_o - the initial solid volume fraction. In all that follows I will restrict the density ρ to be greater than or equal to ρ_o, ν will be required to satisfy the condition $\nu_o \leq \nu \leq 1$, and the magnitude unity constant a° will be deleted for simplicity of notation.

From Eq. (3), the frozen (λ = constant, ν = constant) sound speed is

$$c^2 = \rho - \rho_o \quad . \tag{4}$$

The specific internal energy is

$$e - e_o = -\int_{v_o}^{v} p\,dv' \quad ,$$

in which $v = \frac{1}{\rho}$ is the specific volume. Integration gives

$$e - e_o = \frac{1}{2}(\rho-\rho_o)(1-\rho_o/\rho) - \rho_o \ln(\rho/\rho_o) + \left(\frac{\rho-\rho_o}{\rho\ \rho_o}\right)[\lambda q_1 + (1-A\lambda)(\nu-\nu_o)q_2] \ . \quad (5)$$

Note that Eq. (5) is an equation of state, not a fundamental relation.

The pressures of chemical and mechanical reaction q_1 and q_2, respectively, are assumed to satisfy the inequalities

$$q_1 > 0$$

and (6)

$$q_2 < 0 \ .$$

The first inequality states that the pressure of chemical reaction q_1 is greater than zero. Consider a process at constant ρ and at $\nu = \nu_o$ in which λ goes from 0 to 1. This process increases the pressure from p to $p + q_1$. Thus the chemical reaction adds pressure to the unreacted system at constant ρ and $\nu = \nu_o$. The second inequality states that the pressure of mechanical reaction q_2 is less than zero. Thus a constant density, $\lambda = 0$ change in ν from ν_o to 1, causes a pressure decrease of $(1 - \nu_o)\ q_2$. This simply says that a constant volume decrease in porosity in the unreacted material results in a pressure decrease.[4-6] These results are shown in Fig. 1.

IV. THE STEADY-FRAME AND THE FLOW EQUATIONS

I am interested in the behavior of the material, whose reaction rates and equation of state have been set forth in the preceding sections, as it may vary in steady detonations. As a prelude to the discussion of these detonations I will give precise meaning to the term steady frame by writing down the laboratory frame conservation equations. I then transform them into equations that define the flow in the steady frame. Any flow that satisfies these one-dimensional equations is said to be steady.

In the laboratory frame, the conservation equations of mass, momentum, and energy for an inviscid nonconducting fluid are

$$\rho_t + u\ \rho_2 = -\rho\ u_x \ , \quad (7)$$

$$u_t + uu_x = -\frac{1}{\rho}\ p_x \ , \quad (8)$$

and

$$e_t + u\ e_x = -\ p\ (v_t + u\ v_x) \ , \quad (9)$$

where subscripts indicate partial differentiation with respect to the subscripted variable. D is the velocity of the steady frame in the laboratory; that is,

every discernible feature of the flow in the steady frame travels from left to right with speed D in the laboratory. The head of the flow is at x = 0 at time t = 0, and the steady-frame coordinate is

$$\xi = x - Dt \quad . \tag{10}$$

The transformation does not change t; that is,

$$t \to t \quad . \tag{11}$$

The transformation of the differential operators is given by the chain rule,

$$\frac{\partial}{\partial t})_{\lambda} = \frac{\partial}{\partial t})_{\xi} + (\frac{\partial \xi}{\partial t})_{x} (\frac{\partial}{\partial x})_{t} \tag{12}$$

and

$$\frac{\partial}{\partial x})_{t} = \frac{\partial}{\partial \xi})_{t} \quad ; \tag{13}$$

$(\frac{\partial \xi}{\partial x})_{x}$ is just (-D). When Eqs. (12) and (13) are used in Eqs. (7)-(9), the results are

$$\rho_t - D\rho_\xi + u\rho_\xi = - \rho u_\xi \quad , \tag{14}$$

$$u_t - Du_\xi + uu_\xi = - \frac{1}{\rho} P_\xi \quad , \tag{15}$$

and

$$e_t - De_\xi + ue_\xi = -p(v_t - Dv_\xi + uv_\xi) \quad . \tag{16}$$

Since the frame in which Eqs. (14)-(16) hold is steady, the partial time derivatives are set to zero and the partial space derivatives become total space derivatives. Thus,

$$D \frac{d\rho}{d\xi} = \frac{d(\rho u)}{d\xi} \quad , \tag{17}$$

$$\rho(D - u) \frac{du}{d\xi} = \frac{dp}{d\xi} \quad , \tag{18}$$

and

$$(D - u)\frac{de}{d\xi} = - p(D - u)\frac{dv}{d\xi} \quad . \tag{19}$$

Recall that the equation of state is independent of the internal energy e, and so Eq. (19) will be neglected. Equation (17) may be integrated directly if the particle velocity ahead of the flow is u_o and the density ahead of the flow is ρ_o. Therefore,

$$D(\rho - \rho_o) = \rho u - \rho_o u_o \quad ,$$

which may be rearranged to give

$$\rho(D - u) = \rho_o(D - u_o) \quad . \tag{20}$$

It is possible to integrate Eq. (18) with Eq. (20) so that

$$p - p_o = \rho_o (D - u_o)(u - u_o) \quad . \tag{21}$$

Note that all steady solutions to some specified boundary value problem must satisfy Eqs. (20) and (21). In particular, they are represented in pressure-particle velocity space as straight lines of slope $\rho_o(D-u_o)$. Also, by solving Eq. (20) for u and substituting into Eq. (21), we get

$$p - p_o = \rho_o^2 (D - u_o)^2 (v_o - v) \quad . \tag{22}$$

Thus, like the pressure-particle velocity path, the steady flow lies on a straight line in pressure-specific volume space. This particular equation of a straight line is generally called the Rayleigh Line, and its slope is $-\rho_o^2(D-u_o)^2$.

The rate equations also must be transformed to the steady frame with the results

$$\frac{d\lambda}{d\xi} = - \frac{k_1}{\rho_o(D - u_o)} (1-\lambda)^2 \nu \tag{23}$$

and

$$\frac{d\nu}{d\xi} = - \frac{k_2}{\rho_o(D - u_o)} (1 - \lambda)(1 - \nu) \quad , \tag{24}$$

in which Eq. (20) has been used to replace $\rho(D-u)$ with $\rho_o(D-u_o)$.

Given the reaction rates for λ, and ν, the equation of state relating pressure to density, λ, and ν, and the two steady-flow Eqs. (20) and (22), I have a set of five equations with five unknowns, the pressure p, particle velocity u, density $\rho = \frac{1}{v}$, chemical reaction progress variable λ, and mechanical reaction

progress variable ν. I can now present and solve a one-dimensional steady-flow problem.

V. THE INVISCID DETONATION

The problem considered here is the form of the steady flow at $t = 0$ that results from some boundary motion at $x \ll 0$ and $t \ll 0$. In fact I assume that the distance and time at which the flow began are sufficiently far removed from the present time and position of the flow that any asymptotic processes are changing on a time scale very long with respect to any times during which I examine the system. The head of the flow is now stationary in the steady frame at $\xi = 0$ and the flow extends to negative values of ξ. The head of the flow is occupied by a jump discontinuity in pressure, particle velocity, density, and internal energy through which λ and ν maintain their initial values of 0 and ν_o, respectively. This discontinuity travels with speed D in the laboratory frame. For all values of $\xi < 0$, λ and ν evolve according to Eqs. (23) and (24), which may be solved by forming the equation

$$\frac{d\lambda}{d\nu} = \left(\frac{k_1}{k_2}\right) \frac{(1 - \lambda)}{(1 - \nu)} \nu \quad , \tag{25}$$

which may be integrated directly to give

$$\lambda = 1 - \left[\frac{(1 - \nu)}{(1 - \nu_o)} e^{\nu - \nu_o}\right]^{(k_1/k_2)} \quad . \tag{26}$$

Note that when $\nu = \nu_o$ Eq. (26) gives $\lambda = 0$, whereas when $\nu = 1$, $\lambda = 1$. The function $\lambda = \lambda(\nu)$ given by Eq. (26) is called the reaction path and the λ-ν plane is termed the reaction coordinate phase plane.

The first steady-frame profile to be obtained results from substituting the reaction path into Eq. (24) and integrating; the integral is

$$\int_{\nu_o}^{\nu} \left\{ (1-\nu') \left[\frac{(1-\nu')}{(1-\nu_o)} e^{\nu - \nu_o}\right]^{(k_1/k_2)} \right\}^{-1} d\nu' = - \frac{k_2}{\rho_o (D-u_o)} \int_o^{\xi} d\xi' \quad .$$

A very useful approximation in evaluating this integral is to set $e^{\nu-\nu_o} \simeq 1$. This is satisfactory if $\nu \simeq \nu_o$, that is, $\nu_o \simeq 1$. Thus, I will restrict initial porosity to be $\lesssim 10\%$, which is not a large physical restriction. Note that when $\nu_o = 0.9$, $e^{\nu-\nu_o}$ varies from 1.1 to 1.0 while $(1-\nu)/(1-\nu_o)$ varies from 0 to 1.0. With this approximation incorporated,

$$\nu(\xi) = \frac{\left\{\left[1 - \frac{k_1}{\rho_o (D-u_o)} \xi\right]^{k_2/k_1} - (1-\nu_o)\right\}}{\left[1 - \frac{k_1}{\rho_o (D-u_o)} \xi\right]^{k_2/k_1}} \quad . \tag{27}$$

Note that at $\xi = 0$, $\nu(\xi) = \nu_o$ and $\nu(\xi) \to 1$ as $\xi \to -\infty$.

The next steady-frame profile is obtained by substitution of Eq. (27) into Eq. (23). This results in an equation in λ and ξ that can be directly integrated. The function $\lambda(\xi)$ that results from the integration is

$$\lambda(\xi) = \frac{\left(\frac{k_1}{\rho_o(D-u_o)}\right)\left\{\xi + \left[\frac{1-\nu_o}{k_2/k_1-1}\right]\left[1 - \left(1 - \frac{k_1}{\rho_o(D-u_o)}\,\xi\right)^{(1-k_2/k_1)}\right]\right\}}{1 + \left(\frac{k_1}{\rho_o(D-u_o)}\right)\left\{\xi + \left[\frac{1-\nu_o}{k_2/k_1-1}\right]\left[1 - \left(1 - \frac{k_1}{\rho_o(D-u_o)}\,\xi\right)^{(1-k_2/k_1)}\right]\right\}} . \tag{28}$$

The integration of Eq. (23) after the substitution differs as $k_2 = k_1$ or $k_2 \neq k_1$, leading to a logarithmic integral in the former case. I have chosen to work with $k_2 \neq k_1$. This is not a serious limitation, but it must be observed. Again the limits on $\lambda(\xi)$ are $\lambda(\xi = 0) = 0$, and $\lambda \to 1$ as $\xi \to -\infty$.

To simplify further equations, some initial-state ($\xi > 0$) conditions are set down here. In the initial state, $p_o = 0$, $u_o = 0$, $\lambda = 0$, $\nu = \nu_o$, and $\rho_o = 1$. This assumption will carry over to the viscous case as well.

Now I can calculate the steady-frame pressure profile by eliminating the particle velocity between Eqs. (20) and (21) to yield a single equation in pressure and density. Solving this equation for the density in terms of the pressure and substituting the result into Eq. (3) gives

$$p - \frac{1}{2}\left(\frac{P}{D^2 - P}\right)^2 = \lambda(\xi)q_1 + (1 - A\lambda(\xi))(\nu(\xi) - \nu_o)\, q_2 \quad . \tag{29}$$

The pressure of reaction is

$$p_r = \lambda(\xi)q_1 + (1 - A\lambda(\xi))(\nu(\xi) - \nu_o)\, q_2 \quad . \tag{30}$$

Because this system behaves very differently given differing values of A, I consider the two extremes A = 1 and A = 0 separately.

Case I: A = 1

With A = 1, the system retains no memory in pressure of the mechanical reaction as $\lambda \to 1$. At the end of the reaction zone (that is, $\lambda = 1$ and $\nu = 1$), $p_r = q_1$. Substituting this value into Eq. (29) gives

$$\tilde{p} - \frac{1}{2}\left(\frac{\tilde{p}}{D^2 - \tilde{p}}\right)^2 = q_1 \quad , \tag{31}$$

where $\tilde{p}$ is the particular pressure at the end of the reaction zone. From Eq. (3) the fully reacted equation of state is

$$p = \frac{1}{2}(\rho - \rho_o)^2 + q_1 \quad . \tag{32}$$

The pressure $\tilde{p}$ and the density $\tilde{\rho}$ must satisfy Eq. (32), so

$$\tilde{p} = \frac{1}{2}(\tilde{\rho} - \rho_o)^2 + q_1 \quad . \tag{33}$$

Additionally, since the flow is steady, $\tilde{p}$ and $\tilde{\rho}$ satisfy Eq. (22), giving

$$\tilde{p} = (\rho_o D)^2 (v_o - \tilde{v}) \quad . \tag{34}$$

Equation (34) is a straight line in p-v space that must be tangent to the curve in p-v space given by Eq. (33). This requirement is shown in Fig. 2 as the curve R_o, along with some additional equation-of-state curves for various p_r. To be specific q_1 is assigned the value 0.5.

Figure 2 shows that the Rayleigh Line R_o is the unique solution curve for the given problem. Consider the possibility of R_1 as a solution locus. R_1 intersects the $p_r = 0.5$ locus at two points E and F. Let a nonreactive shock take the system to point G where reaction begins. Suppose reaction is complete at F. The following unsteady flow is a rarefaction into state F traveling with a speed proportional to the slope of the $p_r = 0.5$ locus at F. The wave represented by the line R_1 travels at a speed proportional to its slope, with the proportionality constant the same in both cases. Thus, since the $p_r = 0.5$ locus is steeper at F than at R_1, the advancing rarefaction overtakes the detonation and slows it. The slowing continues until the Rayleigh Line R_o is reached and the rarefaction has precisely the same speed as the detonation, so further degradation by the rarefaction is impossible. The other possibility is that reaction starts at G and is not complete until E is reached on R_1. This violates the condition that the equation of state be satisfied at each point on R_1 when the system is between points F and E; that is, there is no state between F and E on R_1 for which $p_r \leq 0.5$, thus satisfying the equation of state. The Rayleigh Line R_o does, in fact, represent the minimum steady-wave velocity as well. For example, if the solution curve were R_2, the maximum of p_r would be 0.4--again in violation of the correct value. Thus, the locus R_o is the unique steady solution locus.[3] The velocity D with which this flow propagates in the laboratory frame may be calculated directly by setting the slope of the Rayleigh Line $(\rho_o D)^2$ equal to the slope of the $p_r = 0.5$ equation-of-state curve. The resulting cubic equation for p is

$$\tilde{p}^3 - (3q_1 + \tfrac{1}{8})\tilde{p}^2 + q_1(3q_1 + \tfrac{1}{2})\tilde{p} - q_1^2(q_1 + \tfrac{1}{2}) = 0 \quad . \tag{35}$$

With $q_1 = 0.5$, this equation simplifies to

$$2\tilde{p}^3 - 3.25\,\tilde{p}^2 + 2\tilde{p} - 0.5 = 0 \quad ,$$

which yields the solution

$$\tilde{p} = 0.716 \quad .$$

Equation (33) is solved for $\tilde{\rho}$ and gives

$$\tilde{\rho} = 1.6567 \quad .$$

When both $\tilde{p}$ and $\tilde{\rho}$ are substituted into Eq. (34), the result is

$$D = 1.3436 \quad .$$

Recall that $\tilde{p}$ and $\tilde{\rho}$ are the pressure and density at the end of the reaction zone and D is the speed of the steady flow in the laboratory frame.

I have assumed that the pressure suffers a jump discontinuity at $\xi = 0$ to a state on the unreacted $p_r = 0$ equation-of-state locus. Because this discontinuity is a part of the steady flow, it also must propagate with speed D. The intersection of the unreacted equation-of-state locus and the Rayleigh Line R_o is called the ZND point,[3] and detonations in which the ZND point is attained are often called ZND detonations. In this case, the flow is a jump discontinuity to the ZND point followed by a reaction zone of formally infinite extent.

Now, I find the actual pressure profile by solving Eq. (29) for p, given $\lambda(\xi)$, $\nu(\xi)$, and D, at all values of $\xi < 0$. This calculation was performed numerically. I have displayed the results for several values of q_2, k_1, and k_2 in Figs. 3-14. Note that the corresponding $\lambda(\xi)$, $\nu(\xi)$, and $\lambda(\nu)$ plots are also shown.

The first two sets of figures, Figs. 3-6 and 7-10, have a large pressure of mechanical reaction $q_2 = -1000$ with respect to the pressure of chemical reaction, $q_1 = 0.5$. The ZND point is at $p_{ZND} = 1.10$, $\rho_{ZND} = 2.48$, $\lambda = 0$, and $\nu = \nu_o = 0.9$. The plots against distance, ξ, cover four decades on a log scale starting at $\xi = -0.01$ and ending at $\xi = -100$, so the ZND point is not shown but the pressure at that point is shown as the line labeled p_{ZND}. Also included is the line at pressure $p = \tilde{p}$, which is labeled p_{CJ} for the pressure at the Chapman-Jouguet point, which is reached asymptotically.[7]

In Fig. 6 the pressure profile is seen to exceed p_{ZND}. This is because the mechanical reaction is fast enough and the pressure of mechanical reaction sufficiently large that the pressure of reaction p_r becomes negative. Figure 2 shows that the $p_r < 0$ loci are at higher pressures on the Rayleigh Line R_o than the $p_r > 0$ loci. Thus, the total pressure increases from p_{ZND} to a higher value as long as the mechanical reaction dominates. When the chemical reaction begins to quench the mechanical reaction, p_r increases and the system point moves to lower pressures along the Rayleigh Line R_o, going to pressure $\tilde{p} \equiv p_{CJ}$ as $\xi \to -\infty$.

Figures 7-10 show a similar result, except that the magnitudes of the rates are reversed. This causes more rapid quenching of the mechanical rate with a subsequently smaller pressure rise after the initial shock to p_{ZND}. Note the vastly different $\lambda = \lambda(\nu)$ plot.

Figures 11-14 show the approach to a single-reaction ZND detonation. Because q_2 is quite small, the mechanical rate effect is minimal. The overpressure after the initial shock jump is nearly gone and the system approaches $\tilde{p} \equiv p_{CJ}$ much faster than in the previous examples.

Case II. A = 0

When A = 0, which allows complete memory of the mechanical reaction, the problem is more complicated. The function $p_r(\lambda,\nu; A = 0)$ may have a maximum larger than its value at $\lambda = 1$, $\nu = 1$, which occurs at the end of the reaction zone. Consider the flow when $q_2 = -2.5$ and $q_1 = 0.5$. At $\lambda = 1$ and $\nu = 1$,

$$p_r = 0.5 - (.1)(2.5) = 0.25 \quad . \tag{36}$$

Now, let $k_1 = 2$ and $k_2 = 1$; and solve for the extremum of the function

$$p_r = \lambda q_1 + (\nu - \nu_o)\, q_2 \quad , \tag{37}$$

subject to the constraint

$$\lambda = 1 - \left[\left(\frac{1 - \nu}{1 - \nu_o}\right)\, e^{\nu - \nu_o}\right]^{(k_1/k_2)} \quad . \tag{38}$$

Equation (38), the phase plane locus, is valid for all values of A. Taking the derivative of Eqs. (37) and (38) and setting them equal gives

$$\left(\frac{k_1}{k_2}\right) \frac{(1 - \lambda)}{(1 - \nu)}\, \nu = -\left(\frac{q_2}{q_1}\right) \quad . \tag{39}$$

The equivalence of derivatives of the functions $p_r(\lambda)$ and $\nu(\lambda)$ is a tangency condition on these curves. Eliminating λ from Eq. (39) by substitution from Eq. (38) and solving the result gives ν at the extremum of p_r. This is best done iteratively,

$$\nu = 0.9781 \quad . \tag{40}$$

When this value is put into Eq. (38),

$$\lambda = 0.9441 \quad . \tag{41}$$

Finally, p_r at the extremum is found by substituting the above values into Eq. (37).

$$p_r = 0.26767 \quad , \tag{42}$$

which is greater than 0.25 as predicted. The velocity of this steady wave is given by solving Eq. (35) with p_r set to 0.26767.

$$D = 1.1026 \quad . \tag{43}$$

The point in the λ-ν phase plane on the locus of Eq. (38) at which p_r has its extremum is often called the eigenvalue point. A detonation that travels with velocity D given by solution of Eq. (35) with p_r set to its eigenvalue is called an eigenvalue detonation. Figures 15-18 contain the graphs of $\lambda(\xi)$, $\nu(\xi)$, $\lambda(\nu)$, and $p(\xi)$ for this case. A detailed discussion of eigenvalue detonations in a simple context may be found in Ref. 8. Additional discussion of eigenvalue detonations in this system is contained in the Appendix.

VI. THE VISCOUS DETONATION

The main shortcoming of the inviscid assumption is that the system cannot show ignition phenomena. The head of the flow is a shock discontinuity that takes the system discontinuously from its initial state at $\xi > 0$ to an equilibrium thermodynamic state at the head of the shock with no meaningful intervening states. Because there are no definable states of the system within the shock itself, the problem of an ignition condition becomes acute. Real explosives are initiated readily by shocks whose strength is a small fraction of that of the fully developed steady detonations.

To handle this initiation phenomenon in time-dependent calculations, I will solve the viscous steady detonation problem to show the character of the steady viscous flow and its dependence on ignition conditions.

A simple viscous problem can be solved by adding the physical form of the viscous stress to the hydrostatic pressure p to get the total stress.[9] Thus, defining the viscous stress to be

$$\sigma_{VIS} = \eta \frac{du}{d\xi} \text{ , } \eta \text{ a constant} \quad , \tag{44}$$

gives for the total stress

$$\sigma = \eta \frac{du}{d\xi} - p \quad . \tag{45}$$

For the sake of similarity we can define and use a compressive stress as

$$\underline{p} = - \sigma = P - \eta \frac{du}{d\xi} \quad . \tag{46}$$

Note that when $\frac{du}{d\xi} = 0$, $\underline{p} = p$. When $\underline{p}$ replaces p in the equations of motion and the steady-frame equations are rederived, the only change is that $\underline{p}$ replaces p in the results. Thus, Eqs. (21) and (22) become, respectively,

$$\underline{p} - p_o = \rho_o(D - u_o)(u - u_o) \quad , \tag{47}$$

and

$$\underline{p} - p_o = \rho_o^2(D - u_o)^2(v_o - v) \quad . \tag{48}$$

Note that I still have five equations in five unknowns p, ρ, λ, ν, and u. Equation (48) shows that the steady solution in $\underline{p}$-v space is a straight line of slope $\rho_o^2 D^2$, ($u_o = 0$). Thus, the steady viscous flow is governed by the following set of equations;

$$\rho(D - u) = \rho_o D \quad , \tag{49}$$

$$\eta \frac{du}{d\xi} = p - \rho_c^2 D^2(v_o - v) \quad , \tag{50}$$

$$\frac{d\lambda}{d\xi} = -\left(\frac{k_1}{\rho_o D}\right)(1-\lambda)^2 \nu \quad , \tag{51}$$

$$\frac{d\nu}{d\xi} = -\left(\frac{k_2}{\rho_o D}\right)(1-\lambda)(1-\nu) \quad , \tag{52}$$

and

$$p = \frac{1}{2} a^o(\rho - \rho_o)^2 + \lambda q_1 + (1 - A\lambda)(\nu - \nu_o)\, q_2 \quad . \tag{53}$$

Equation (53) may be used in Eq. (50) to eliminate p as a function of ρ, λ, and ν. Equation (49) may then be used to replace ρ and v in Eq. (50) with a function of u. Thus, I am left with three equations in the three dependent variables u, λ, and ν with parameters η, k_1, k_2, q_1, q_2, A, ν_o, ρ_o, and D. This system of coupled ordinary differential equations, (50)-(52), can be solved numerically when the material parameters and D are specified. Also, I can manipulate ignition conditions. For example, if I want a pressure-dependent ignition criterion, I set up the conditions

$$\eta \frac{du}{d\xi} = f(u,\ \lambda = 0,\ \nu = \nu_o) \quad , \tag{54}$$

$$\frac{d\lambda}{d\xi} = 0 \quad , \tag{55}$$

and

$$\frac{d\nu}{d\xi} = 0 \quad , \tag{56}$$

until $p \geq p_{ig}$ (p_{ig} is ignition pressure). When $p \geq p_{ig}$, the zero rate requirements are removed.[6] Another example with more interesting physical possibilities is to require ν to advance to some point between ν_o and 1, say ν^*, before the chemical rate is turned on;

$$\eta \frac{du}{d\xi} = f(u,\ \lambda,\ \nu) \quad , \tag{57}$$

$$\frac{d\nu}{d\xi} = \begin{cases} 0 \text{ for } p < p_{ig} \\ -\left(\dfrac{k_2}{\rho_o D}\right)(1-\lambda)(1-\nu) \text{ for } p \geq p_{ig} \end{cases} \quad , \tag{58}$$

and

$$\frac{d\lambda}{d\xi} = \begin{cases} 0 \text{ for } \nu_o \leq \nu < \nu^* \\ -\left(\frac{k_1}{\rho_o D}\right)(1-\lambda)^2 \nu \text{ for } \nu \geq \nu^* \end{cases} . \tag{59}$$

There is no limit to the possibilities that now exist for igniting the system.

To proceed with an actual calculation, one must find D for given material parameters. The calculation of the wave speed proceeds exactly as it did in Sec. IV, except for the ability to turn on the rates independently, which does not alter the general technique outlined in Sec. IV. I will again consider A = 0 and A = 1 separately.

Case III. A = 1, Viscous Flow

This discussion concerns the ignition condition set out in Eqs. (57)-(59). This leads to enough complication and provides a good look at the trickery required to solve this and similar problems.

Equations (58) and (59) show that I can integrate Eq. (58) from $\nu = \nu_o$ to $\nu = \nu^*$ because, over these values of ν, $\lambda = 0$. The result is

$$\nu = 1 - [(1-\nu_o)\, e^{(\frac{k_2}{\rho_o D})\xi}], \quad \nu_o \leq \nu < \nu^* . \tag{60}$$

When ν becomes equal to ν^*, Eq. (59) is turned on and the phase plane locus is found as the solution of

$$\frac{d\lambda}{d\nu} = \left(\frac{k_1}{k_2}\right) \frac{(1-\lambda)}{(1-\nu)} \nu , \tag{61}$$

in which as λ moves from 0 to 1, ν moves from ν^* to 1. Integrating Eq. (61) directly gives

$$\lambda = 1 - \left[\left(\frac{1-\nu}{1-\nu^*}\right) e^{\nu-\nu^*}\right]^{(k_1/k_2)} . \tag{62}$$

Note the similarity to Eq. (26). As in Sec. IV, assume that $e^{\nu-\nu^*} \cong 1$. Figure 19 shows the λ-ν phase plane loci of Eqs. (62) and (26) when $k_1 \cong k_2$ and $\nu^* = 0.93$. The differences are apparent.

First I examine the case for A = 1; the system retains no memory of the mechanical dissipation occurring as both reactions move to completion. In fact, the maximum value of p_r is $q_1 = 0.5$. Further, at the point in $\underline{p}$ - v space where the straight line of Eq. (48) is tangent to the $p_r = 0.5$ equation-of-state locus, it is assumed that $\underline{p} = p$. Thus, the value obtained for D is precisely that found for case I, Sec. V,

$$D = 1.3436 . \tag{63}$$

With D known, solutions of Eqs. (50)-(52) (subject to the given ignition condition) are readily obtained. I have written a short computer program using the FTNMATH subroutine ODE to solve this particular problem. The figures described below contain the results of several calculations with various values of k_1, k_2, q_2, ν^*, and η. The figure captions contain the information about the material that pertains to the given calculation. Note that these sets of figures result when A = 1.

The Figures for Case III

Figures 20-23. The material parameter values are A = 1, q_1 = 0.5, q_2 = -1.0, k_1 = 10, k_2 = 10, and η = 0.01. The plot of primary interest is that of $\nu - \nu_o$ vs λ. Note that $\nu - \nu_o$ increases to $\sim$0.03 before any chemical reaction occurs. When the chemical reaction begins, note that $\nu - \nu_o$ varies approximately linearly in λ. The plot of pressure and stress vs distance is also noteworthy in that the system is only slightly viscous, η = 0.01, so the stress and pressure are approximately equal even in early parts of the wave.

Figures 24-27. The material parameter values are A = 1, q_1 = 0.5, q_2 = -10.0, k_1 = 10, k_2 = 10, and η = 0.01. These figures show the result of changing q_2 by an order of magnitude. The only really discernible change from Figs. 20-23 is the slight increase in peak pressure and stress, which is a result of more mechanical reaction pressure during the middle stages of the mechanical reaction.

Figures 28-31. The material parameter values are A = 1.0, q_1 = 0.5, q_2 = -10.0, k_1 = 10, k_2 = 2, and η = 0.01. I have decreased k_2 by half an order of magnitude. Note that the $\nu - \nu_o$ vs λ plot shows λ increasing relatively faster than $\nu - \nu_o$. Also, the pressure and stress vs distance shows an increasing ramp near the peak because the retarded mechanical rate allows a longer pressure buildup before the ignition of the chemical rate, which subsequently lowers the pressure. Note that the first bend in the pressure profile coincides with the ignition of the mechanical reaction, whereas the peak in the pressure profile coincides with the ignition of the chemical reaction, in agreement with the foregoing discussion.

Figures 32-35. The material parameter values are A = 1.0, q_1 = 0.5, q_2 = -10.0, k_1 = 10, k_2 = 2, and η = 0.10. This figure demonstrates the effects of varying the viscosity parameter η, which has been increased by an order of magnitude. The $\nu - \nu_o$ vs λ plot is unaltered because η does not appear in the phase plane equation. However, the graph of pressure and stress vs distance is altered considerably. The stress peaks at the same value but at a greater distance than it did in Figs. 28-31. The pressure, however, peaks at a higher value because the viscous stress σ_{VIS} becomes positive after the stress peak. Note that when $dP/d\xi = 0$ the pressure locus crosses the $\underline{p}$ locus as it should. This would not occur if a viscous stress were incorporated only in compression to handle sharp shocks rather than as a real material property.

Finally, the effect of the increased viscosity on λ vs distance and $\nu-\nu_o$ vs distance plots shifts the onset of both reactions away from the origin.

Figures 36-39. The material parameter values are A = 1.0, q_1 = 0.5, q_2 = -10.0, k_1 = 10, k_2 = 10, and η = 0.10. I have returned k_2 to 10 in this highly viscous calculation. The primary change is in the $\nu-\nu_o$ vs λ phase plane, as expected. Note also that the slight pressure overshoot shown in Fig. 39 remains,

though it is not so large as that shown in Fig. 35 because the chemical rate is turned on earlier than it was in the previous figure. Recall that a slow mechanical rate retards the chemical rate and moves the chemical rate ignition point away from the origin.

Case IV. A = 0.0, Viscous Flow

I will now discuss the extension of Case II to viscous flow. Because A = 0 the system retains complete memory of the pressure of mechanical reaction. Recall that I am using the ignition condition set out in Eqs. (57)-(59). The primary result of interest is that, besides forming eigenvalue detonations caused only by memory of the mechanical reaction as in Case II, the ignition condition also influences the location of the eigenvalue point. That is, a material's ignition, according to Eqs. (57)-(59), leads to different detonation velocities as the value of ν^* is altered. This behavior can occur for any value of A such that $0 \leq A < 1$.

The change in detonation velocity as influenced by changes in ν^* is shown in Fig. 40, the $(\nu-\nu_o) - \lambda$ phase plane. Two reaction loci are shown with three p_r = constant loci. Curve 1 is a reaction path for $\nu^* = 0.905$, and curve 2 is a reaction path for $\nu^* = 0.92$. The p_r = constant loci are given by

$$\lambda = \frac{p_r - (\nu-\nu_o)\, q_2}{q_1} \quad . \tag{64}$$

These are simply straight lines of slope (q_2/q_1) and λ intercept p_r/q_1 in the $\lambda - (\nu-\nu_o)$ phase plane. The three p_r = constant loci are, respectively, a tangent to 1, a tangent to 2, and the $p_r = 0.0$ locus. Note that $p_r(1) > p_r(2)$, so the detonation velocity corresponding to ignition at $\nu^* = 0.905$ is greater than that corresponding to ignition at $\nu^* = 0.92$, although the material parameters for both are identical. Decreasing the value of $|q_2|$ relative to q_1 decreases the slope of the p_r curves and will lead to greater differences in detonation velocity for a given change in ignition point.

I have made a pair of calculations with $k_1 = 5$, $k_2 = 2.5$, $q_1 = 0.5$, $q_2 = -2.5$, $A = 0.0$, and $\eta = 0.01$. In the first, $\nu^* = 0.905$, and in the second, $\nu^* = 0.92$. The results are displayed in Figs. 41-44 and 45-48.

VII. CONCLUSIONS

This analysis of the steady waves possible in a simple porous-reactive analog with asymptotic rates has shown much of the behavior of similar systems.[8] In viscous flow, both the wave profiles and the detonation velocity are affected by the ignition condition. The dominant eigenvalue detonation in cases II and IV suggests that when an endothermic reaction accompanies an exothermic reaction one could observe this phenomenon. Some control over the degree of endothermicity would be useful.

The remaining area of interest is the system's behavior during the initiation and buildup to detonation. Simple boundary conditions such as constant pressure boundaries will be used to check the purely porous (dissipative) response, the purely chemical response, and mixtures thereof. System initiation will be simulated by short-shock flyer plate impact to compare the analog with a genuine explosive such as PBX-9404.

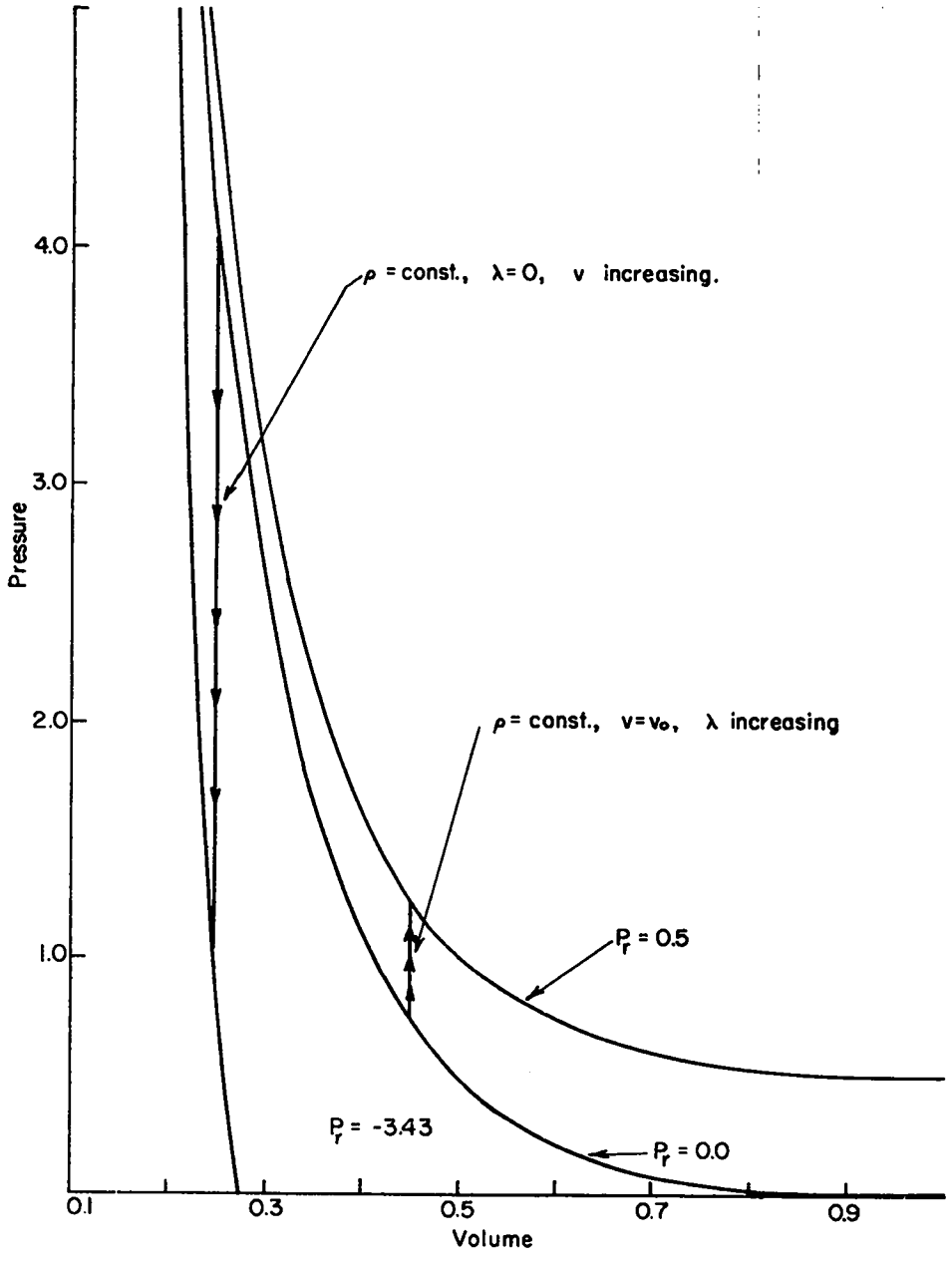

Fig. 1. The equation of state and some representative processes.

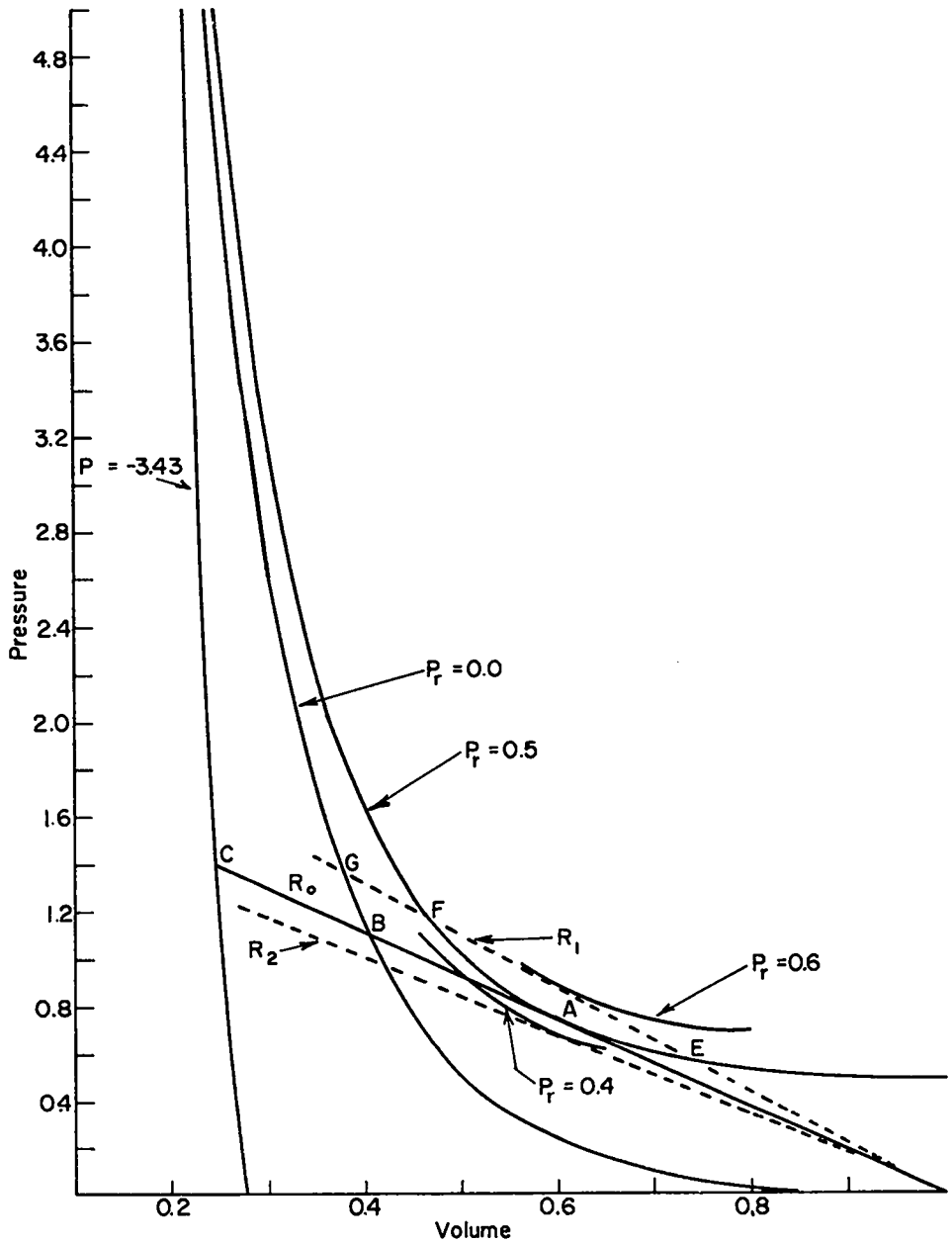

Fig. 2. A pictorial representation of the Chapman-Jouguet hypothesis.

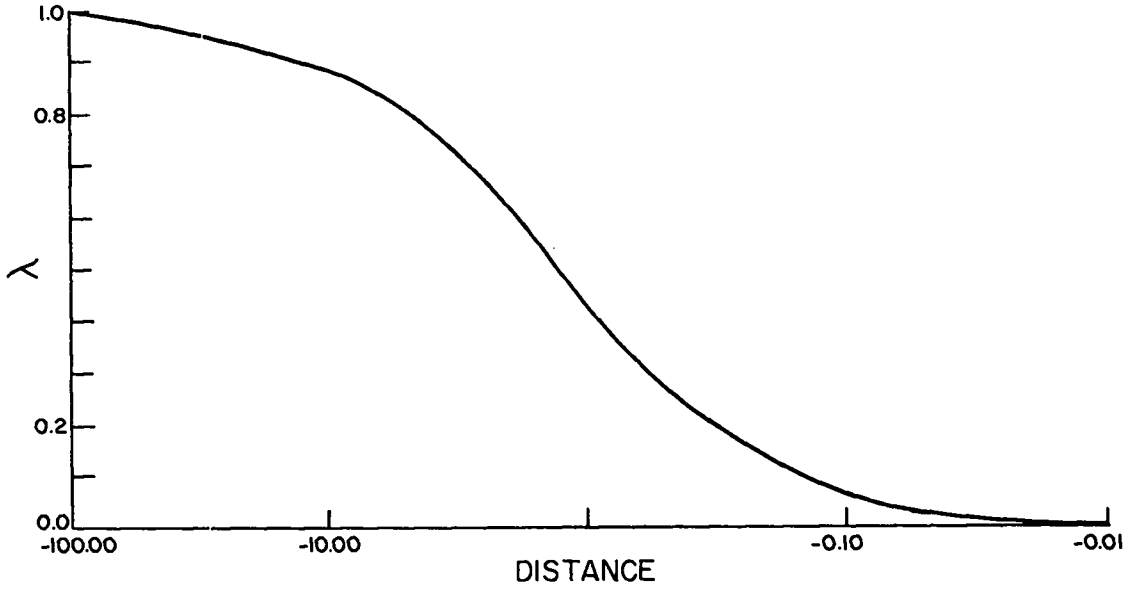

Fig. 3. Reaction extent λ vs distance.

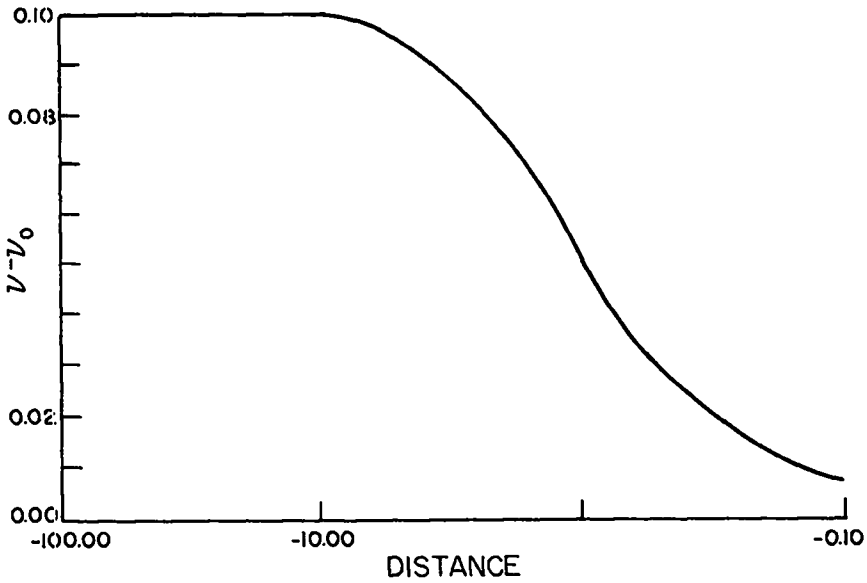

Fig. 4. Reduced solid volume fraction $\nu-\nu_o$ vs distance.

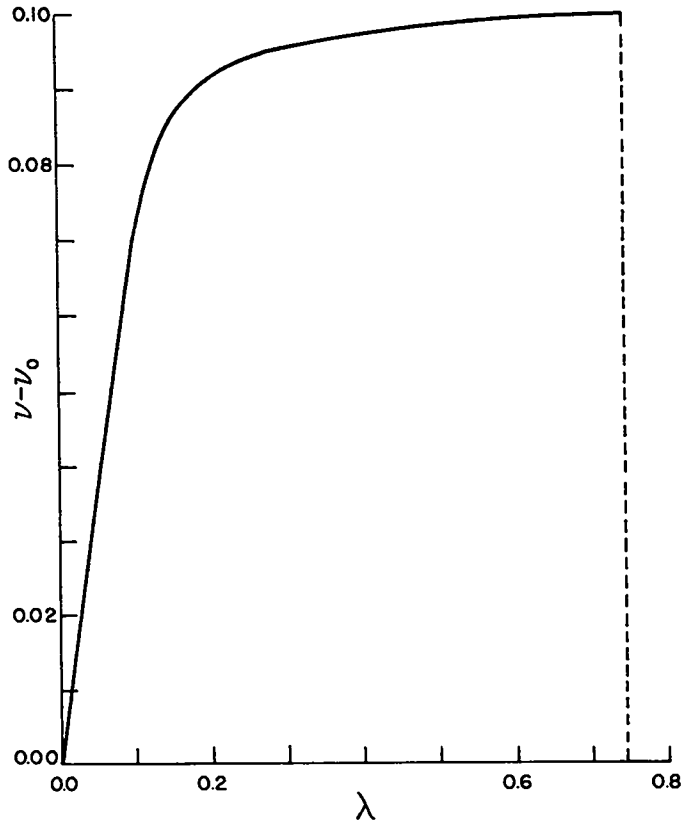

Fig. 5. Reduced solid volume fraction $\nu-\nu_o$ vs reaction extent λ.

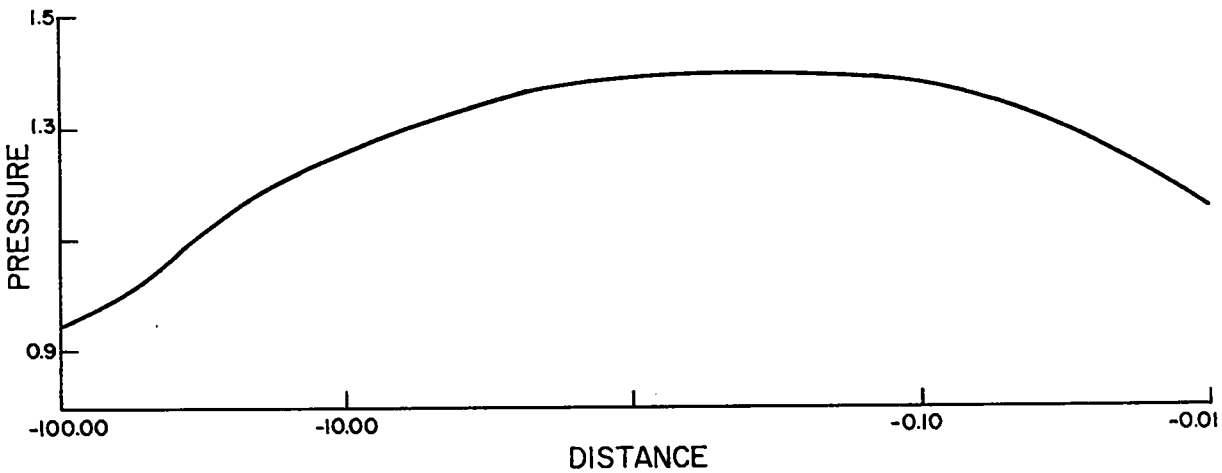

Fig. 6. Pressure vs distance.

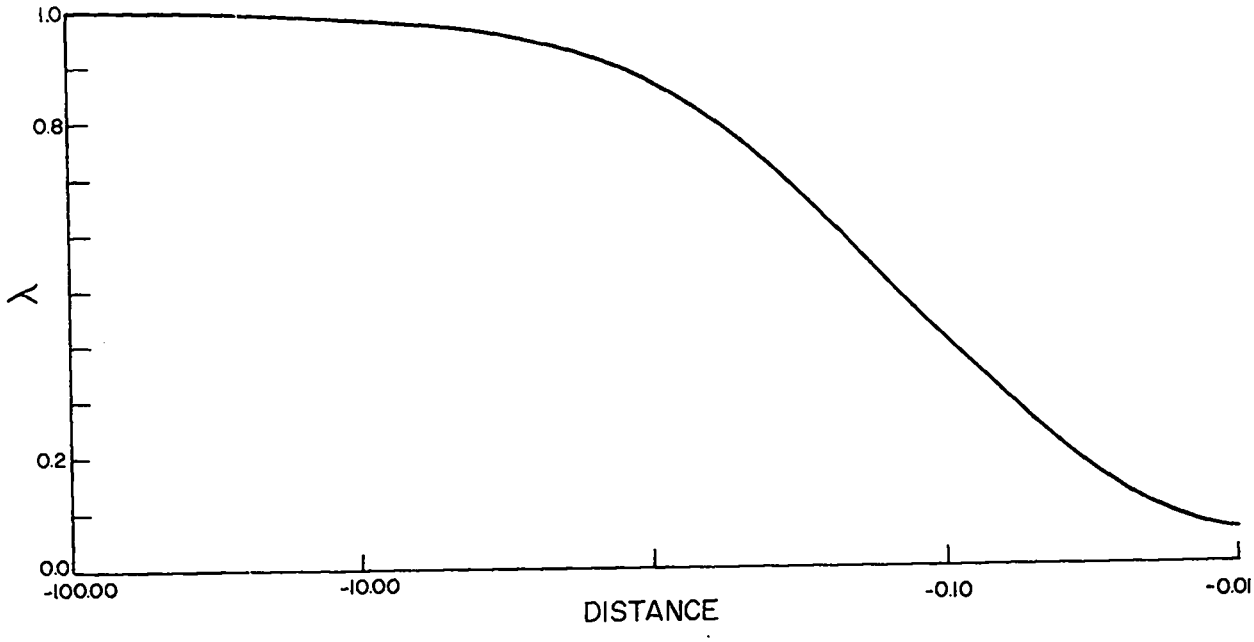

Fig. 7. Reaction extent λ vs distance.

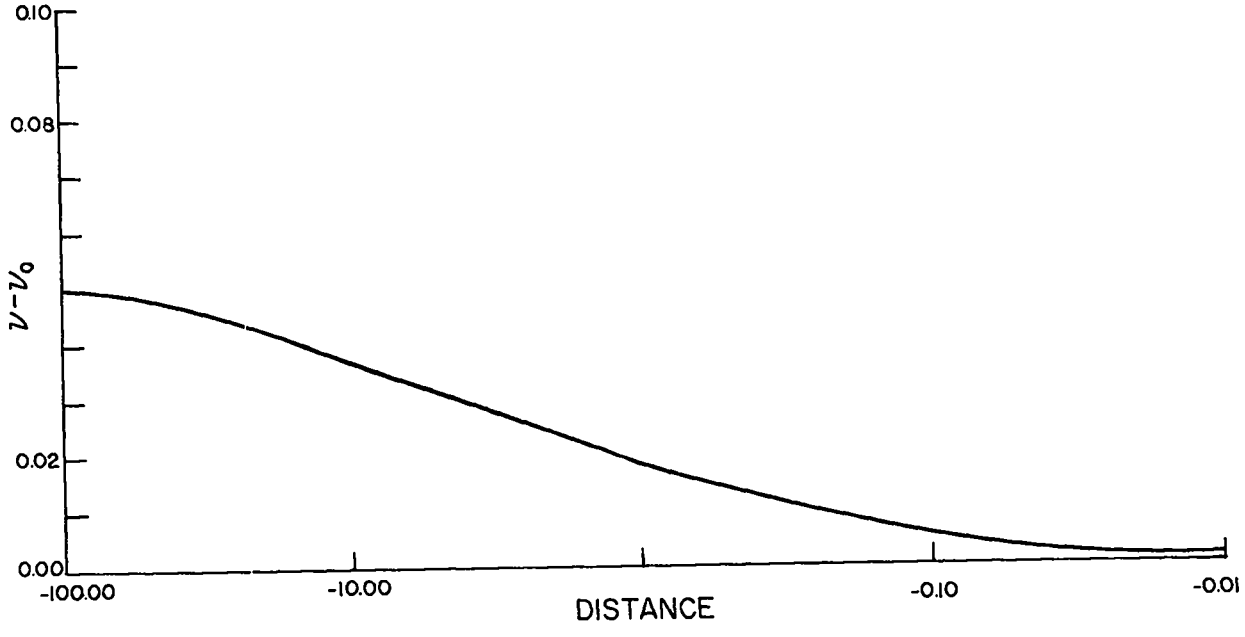

Fig. 8. Reduced solid volume fraction $\nu-\nu_o$ vs distance.

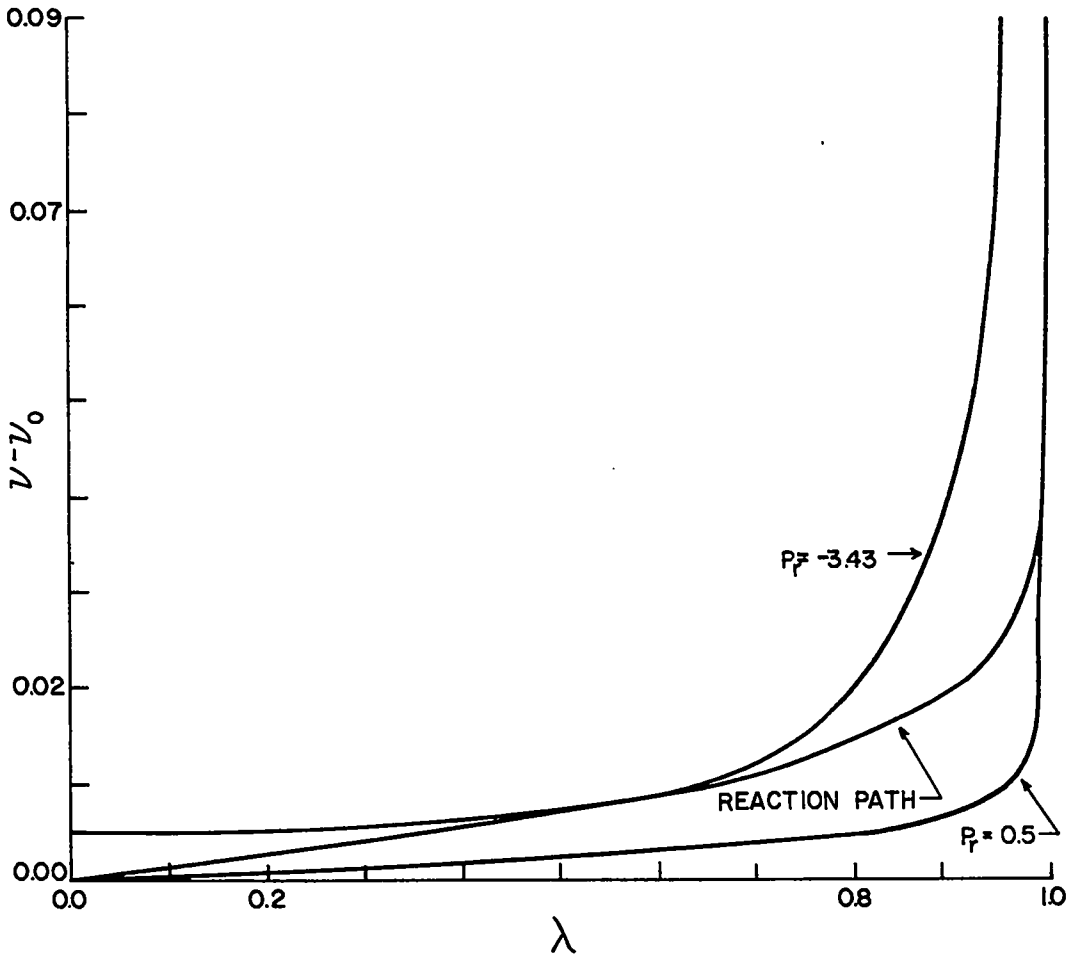

Fig. 9. Reduced solid volume fraction $\nu-\nu_o$ vs distance with both extrema of p_r shown.

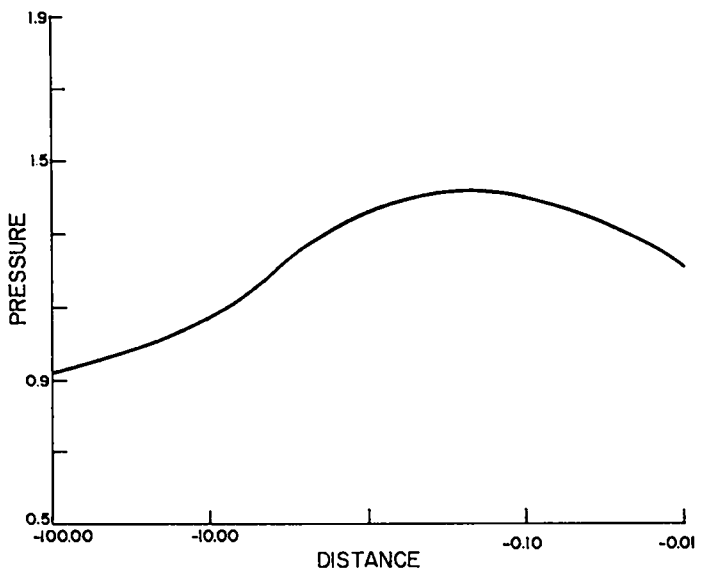

Fig. 10. Pressure vs distance.

Fig. 11. Reaction extent λ vs distance.

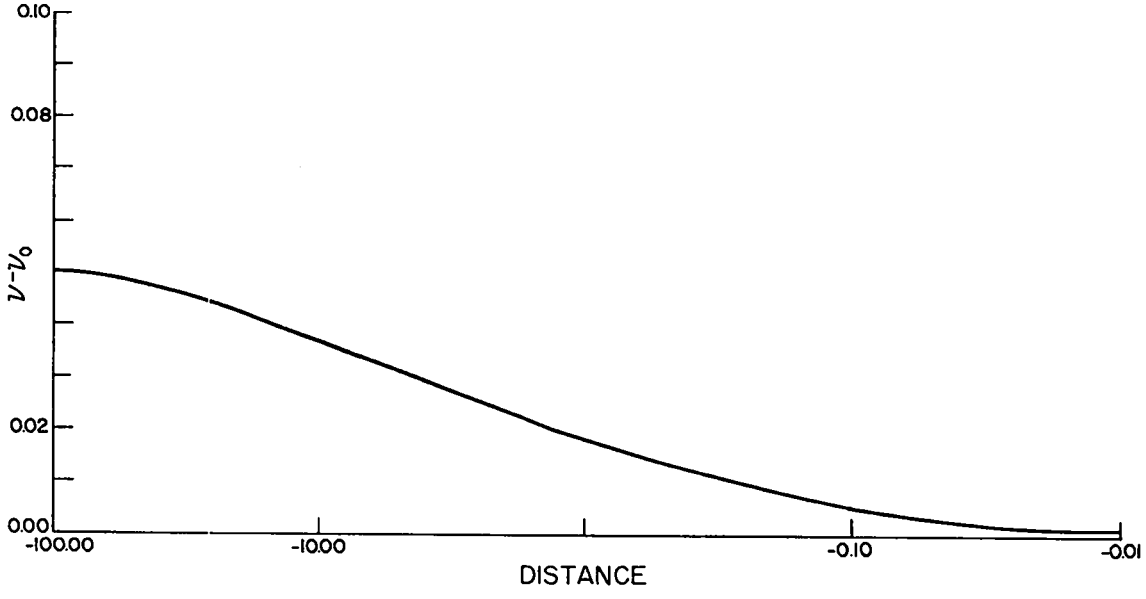

Fig. 12. Reduced solid volume fraction $\nu-\nu_o$ vs distance.

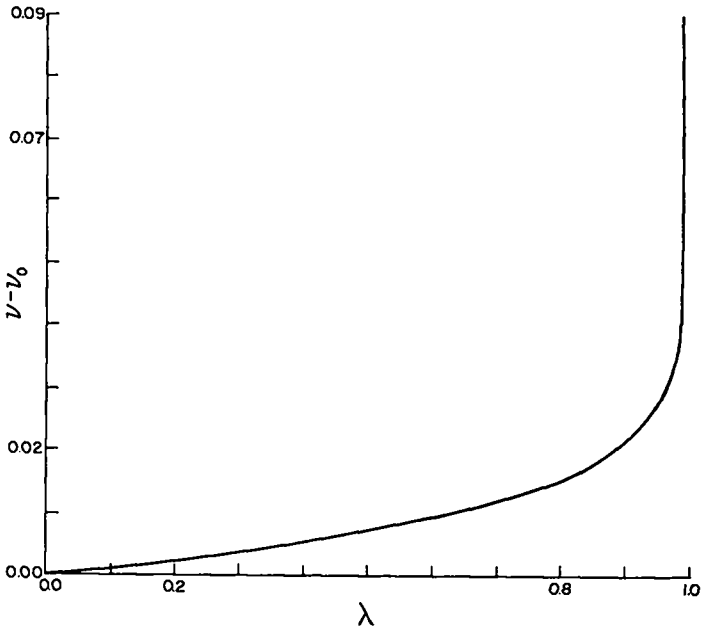

Fig. 13. Reduced solid volume fraction $\nu-\nu_o$ vs reaction extent λ.

Fig. 14. Pressure vs distance.

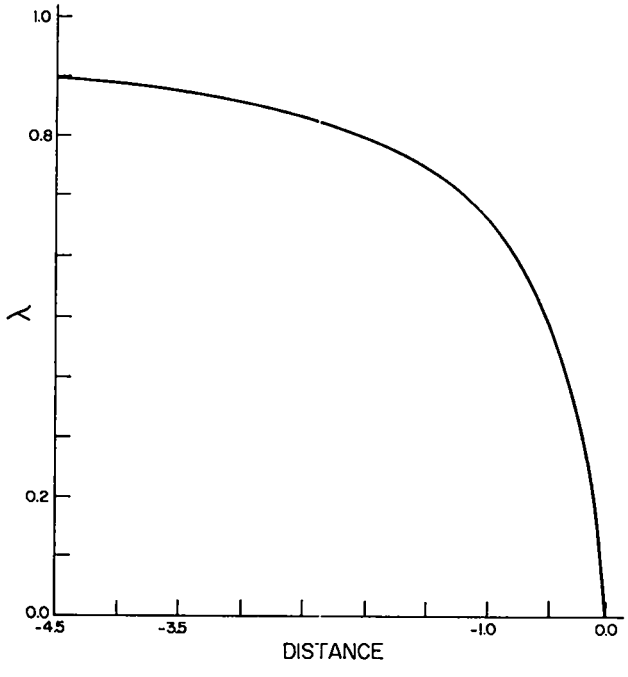

Fig. 15. Reaction extent λ vs distance.

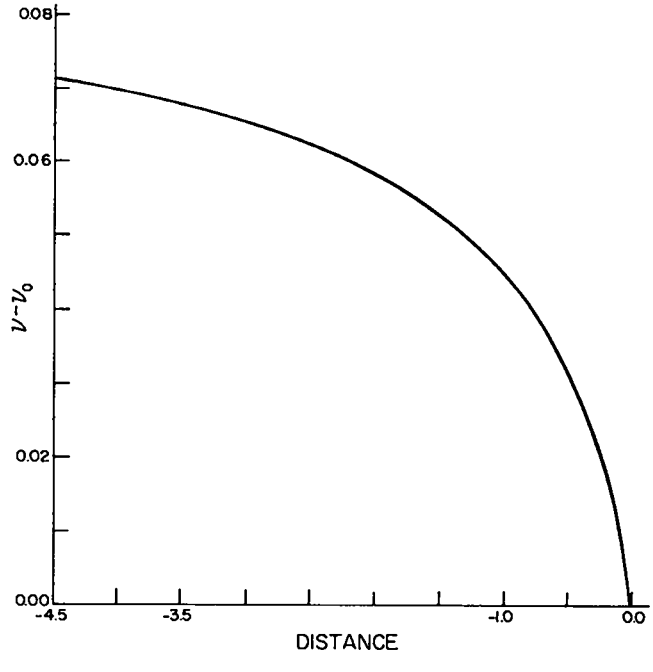

Fig. 16. Reduced volume fraction $\nu-\nu_o$ vs distance.

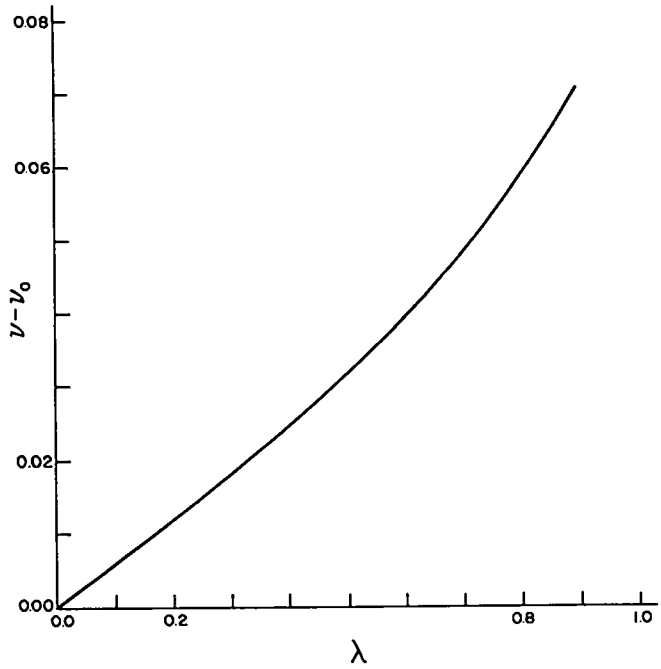

Fig. 17. Reduced volume fraction $\nu-\nu_o$ vs reaction extent λ.

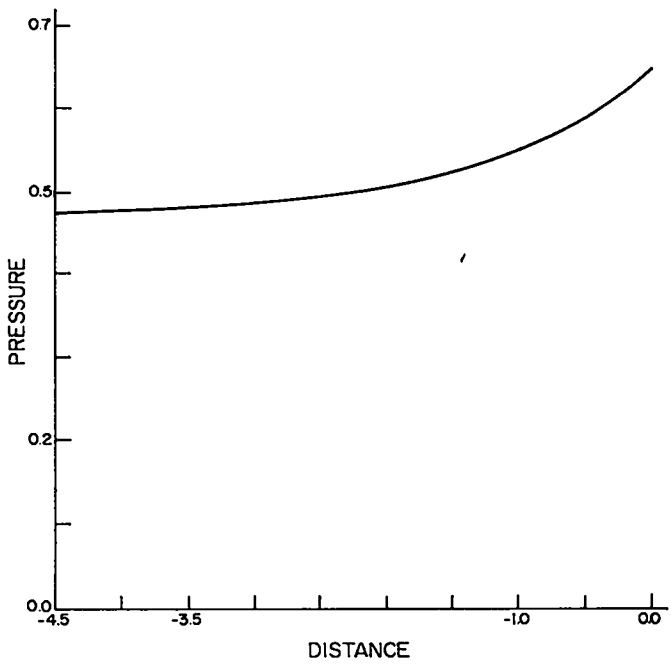

Fig. 18. Pressure and stress vs distance.

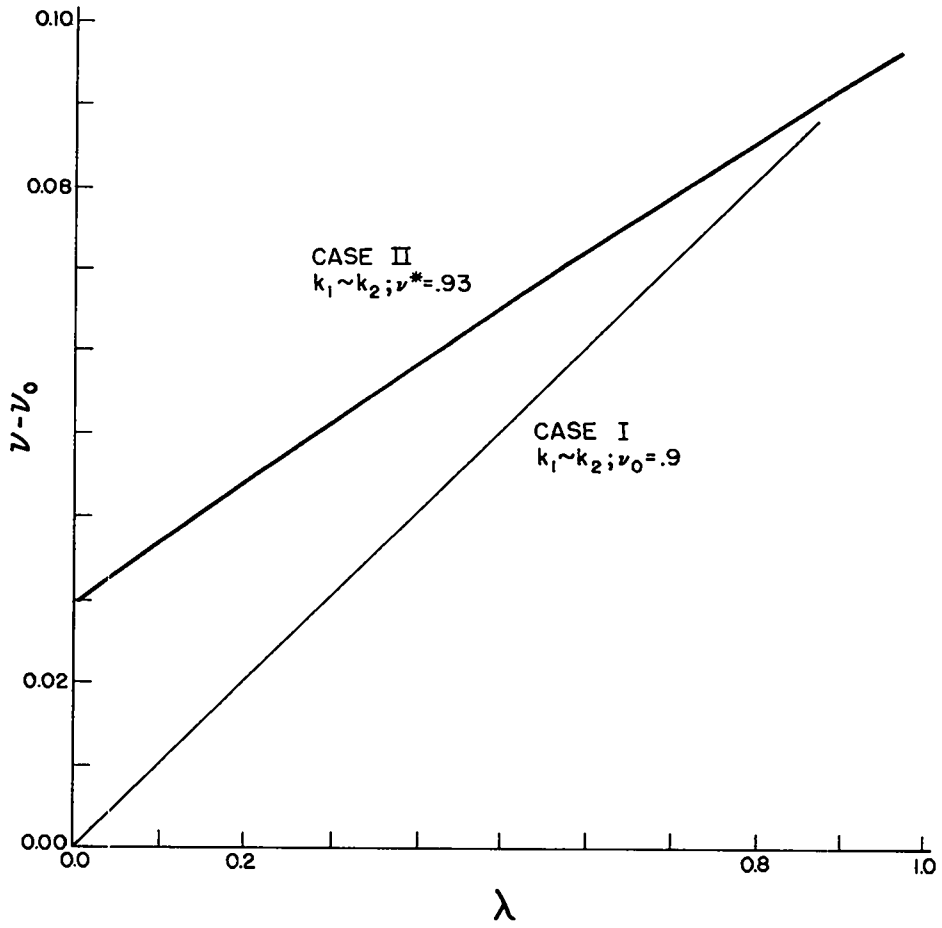

Fig. 19. The result of changing ν^* on the reduced volume fraction $\nu-\nu_o$ vs reaction extent λ loci in the $(\nu-\nu_o)$ - λ phase plane.

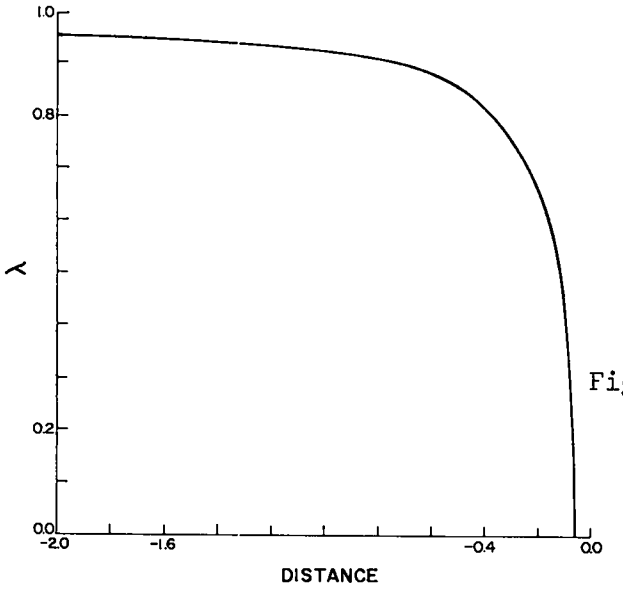

Fig. 20. Reaction extent λ vs distance.

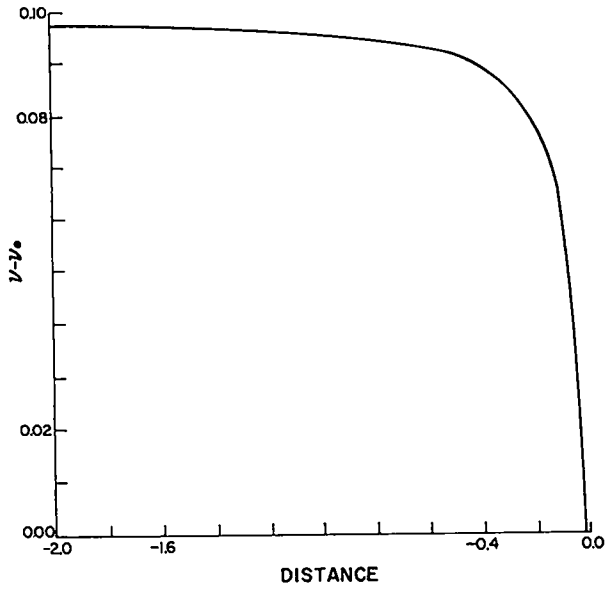

Fig. 21. Reduced volume fraction $\nu-\nu_o$ vs distance.

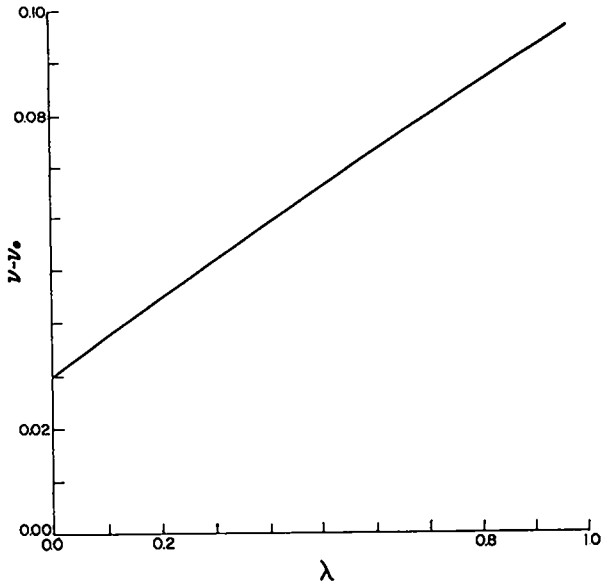

Fig. 22. Reduced volume fraction $\nu-\nu_o$ vs reaction extent λ.

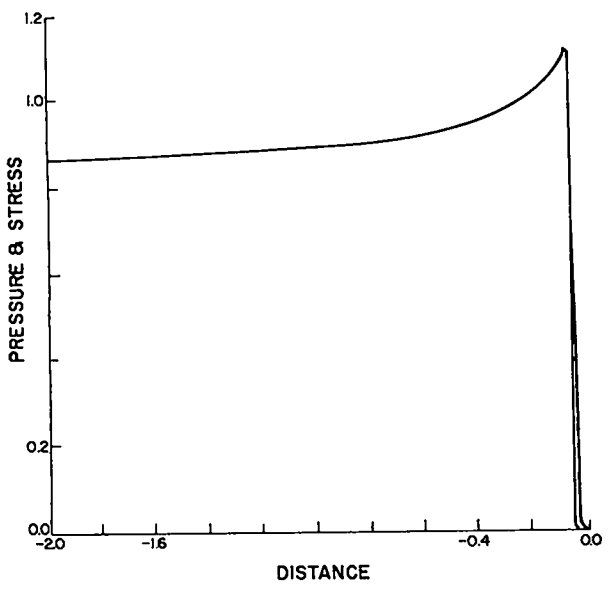

Fig. 23. Pressure and stress vs distance.

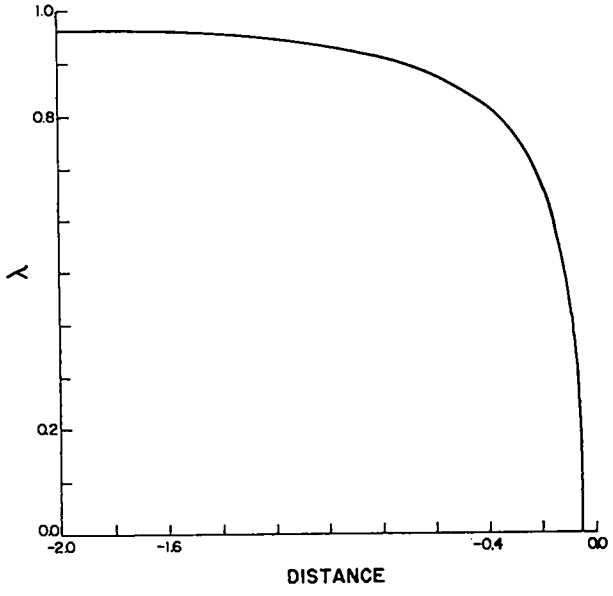

Fig. 24. Reaction extent λ vs distance.

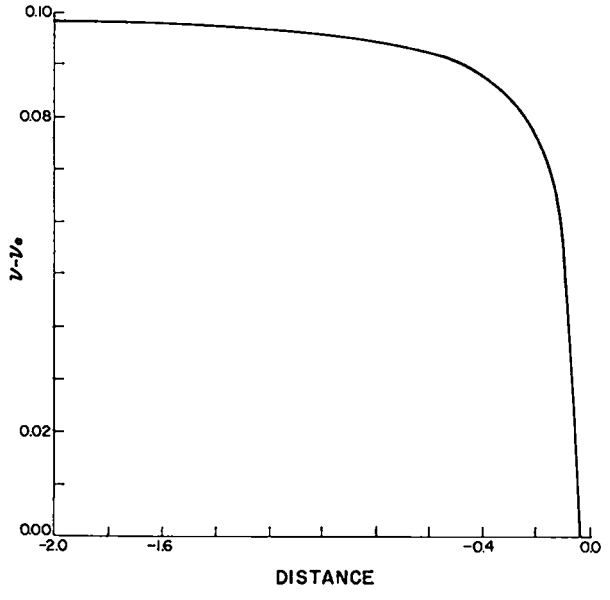

Fig. 25. Reduced volume fraction $\nu-\nu_o$ vs distance.

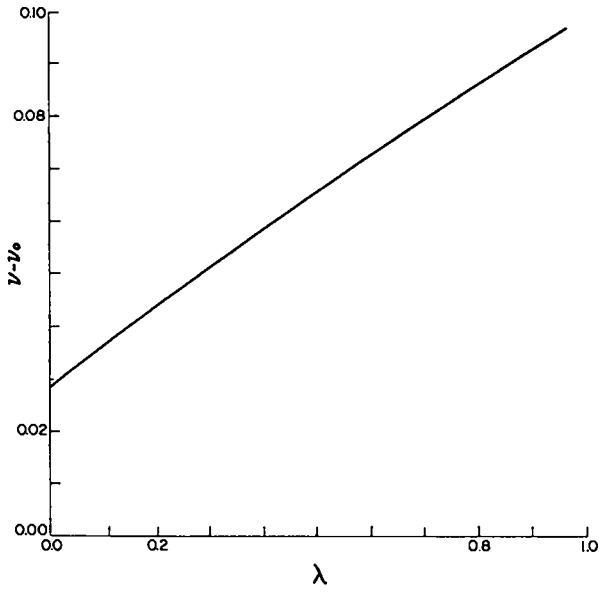

Fig. 26. Reduced volume fraction $\nu-\nu_o$ vs reaction extent λ.

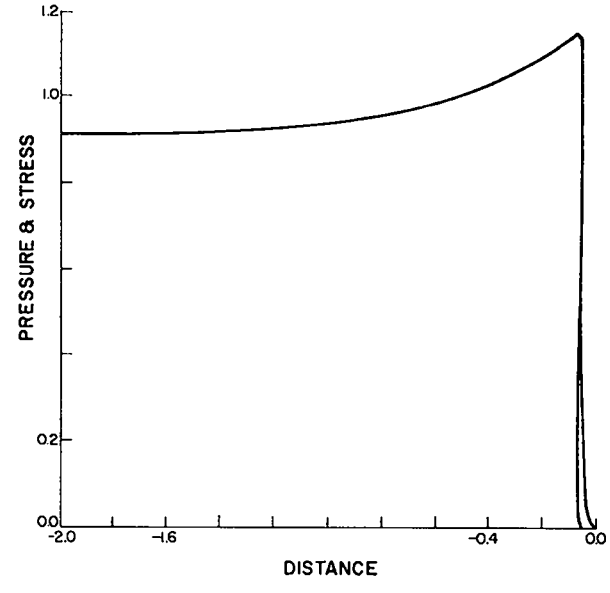

Fig. 27. Pressure and stress vs distance.

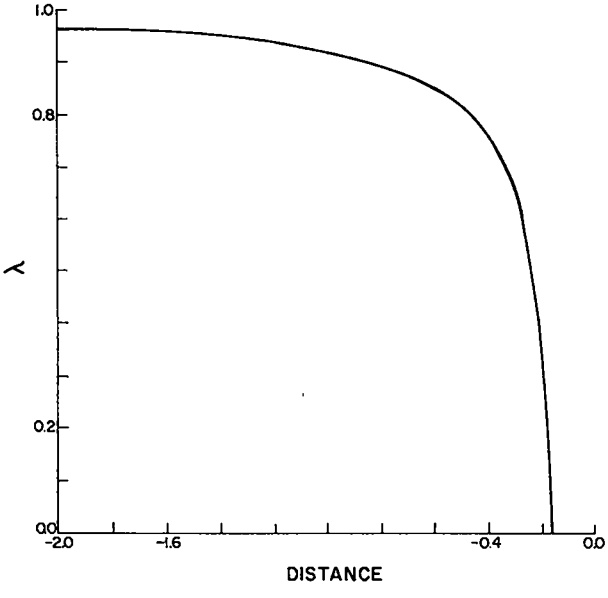

Fig. 28. Reaction extent λ vs distance.

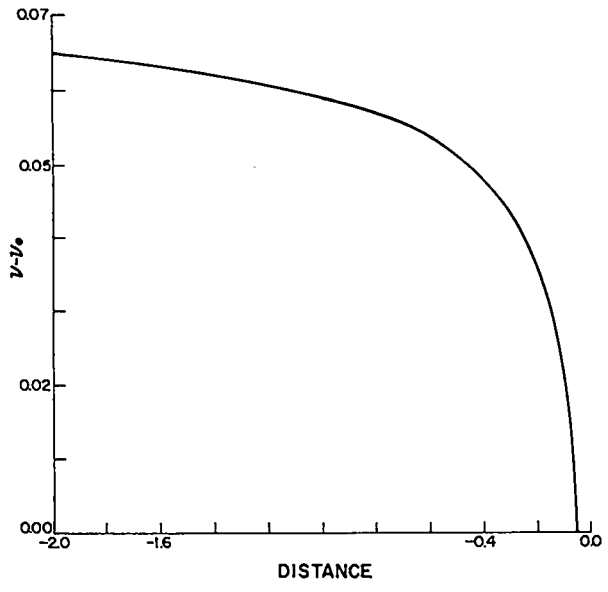

Fig. 29. Reduced volume fraction $\nu-\nu_o$ vs distance.

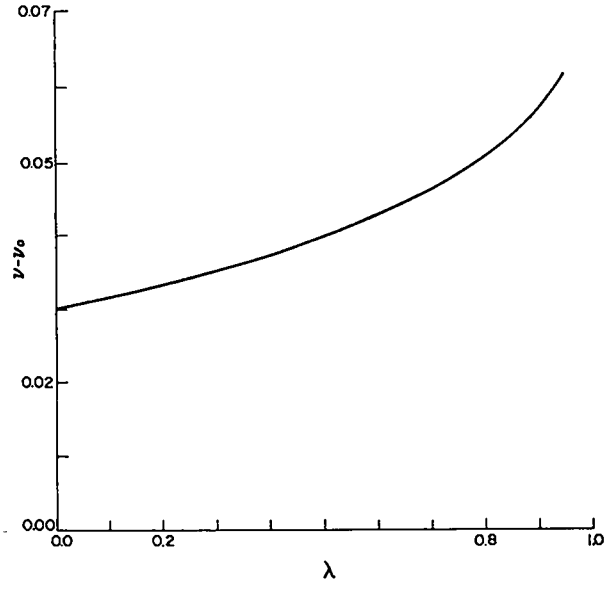

Fig. 30. Reduced volume fraction $\nu-\nu_o$ vs reaction extent λ.

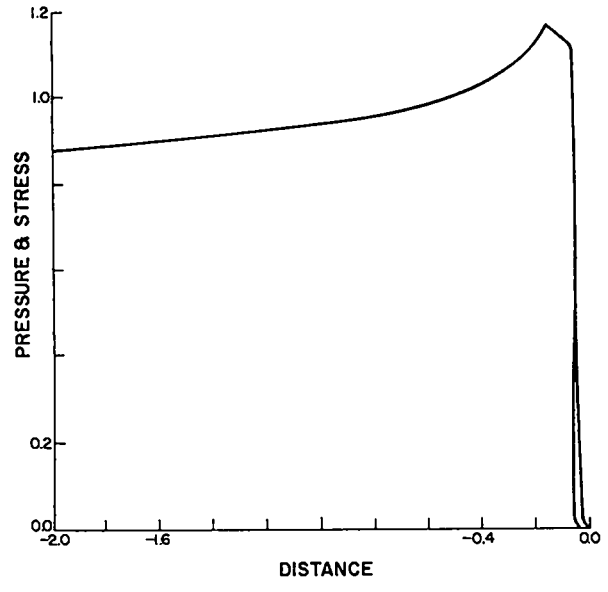

Fig. 31. Pressure and stress vs distance.

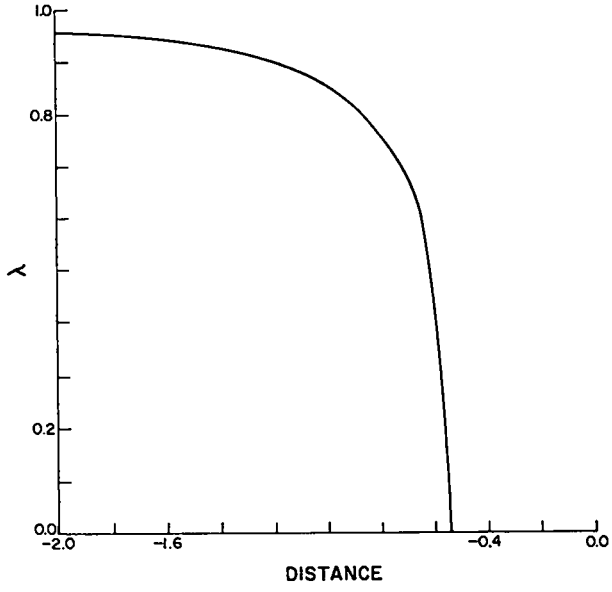

Fig. 32. Reaction extent λ vs distance.

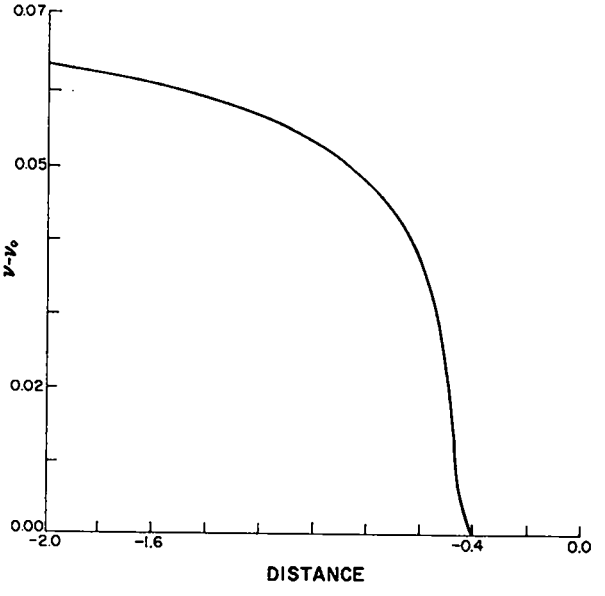

Fig. 33. Reduced volume fraction $\nu-\nu_o$ vs distance.

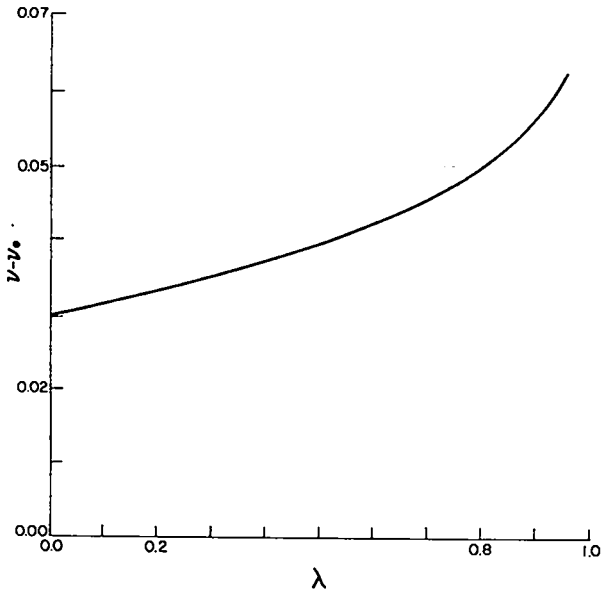

Fig. 34. Reduced volume fraction $\nu-\nu_o$ vs reaction extent λ.

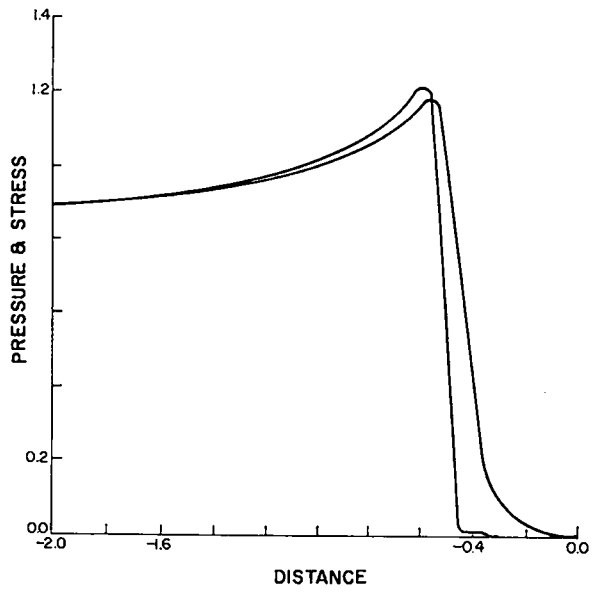

Fig. 35. Pressure and stress vs distance.

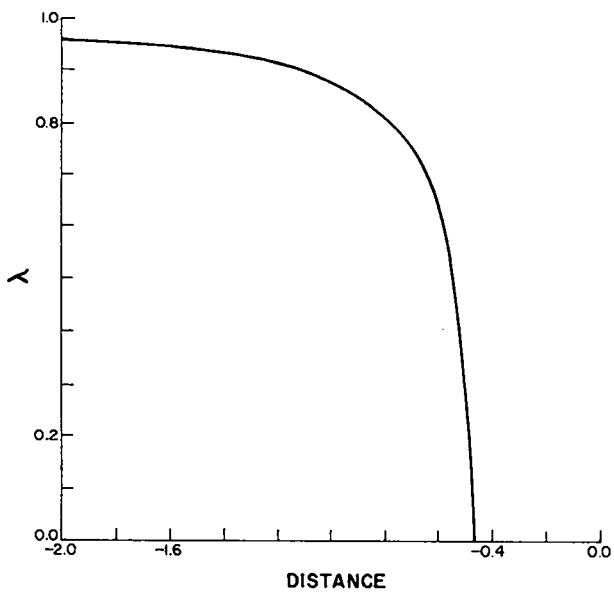

Fig. 36. Reaction extent λ vs distance.

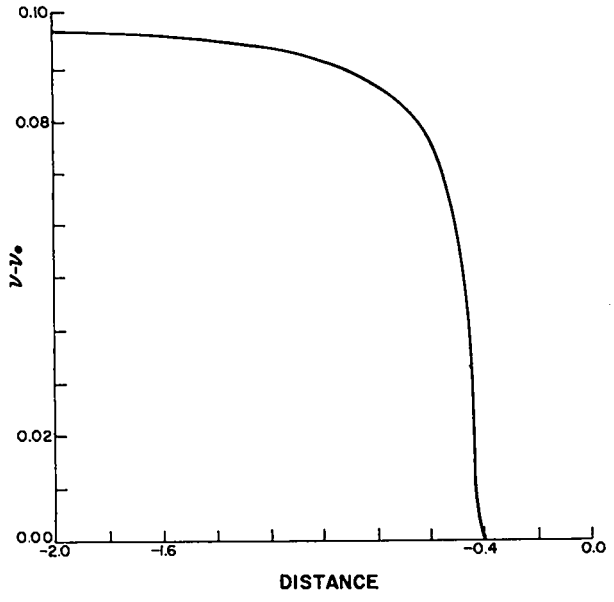

Fig. 37. Reduced volume fraction $\nu-\nu_o$ vs distance.

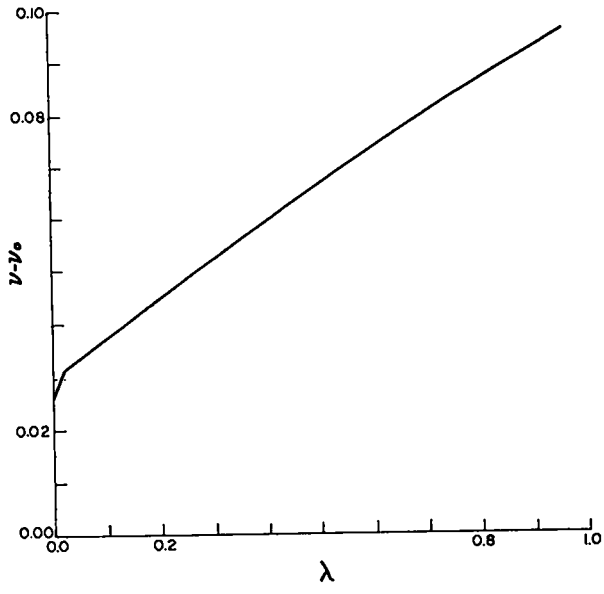

Fig. 38. Reduced volume fraction $\nu-\nu_o$ vs reaction extent λ.

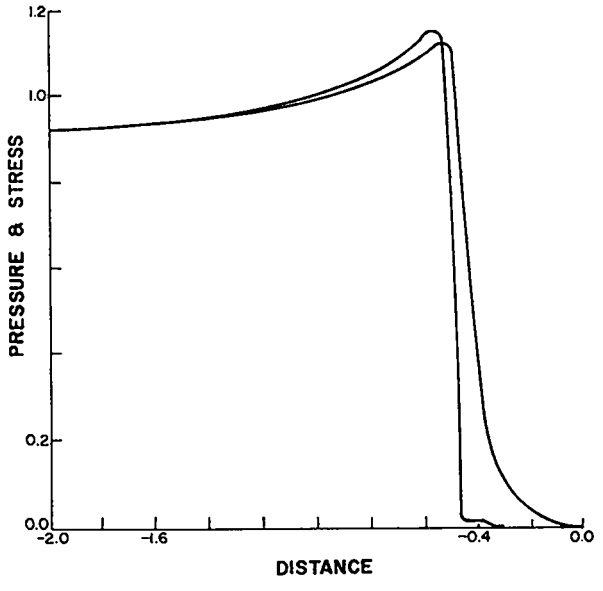

Fig. 39. Pressure and stress vs distance.

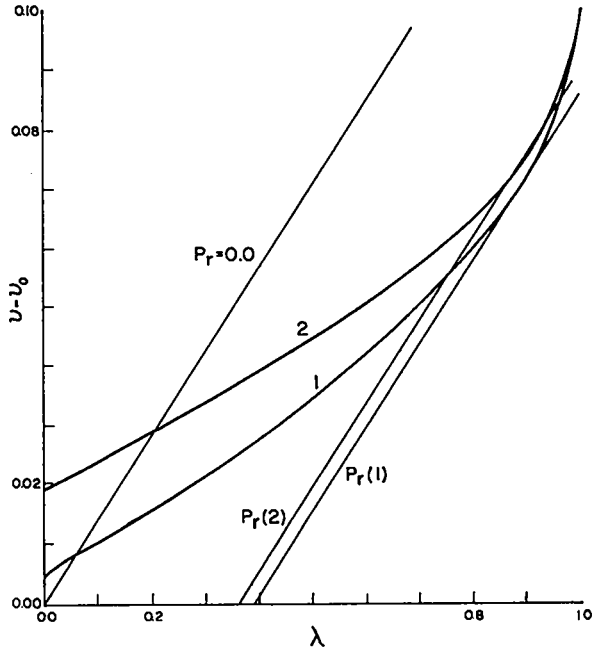

Fig. 40. A graphical representation of the change in detonation velocity as it depends on the ignition point ν^*.

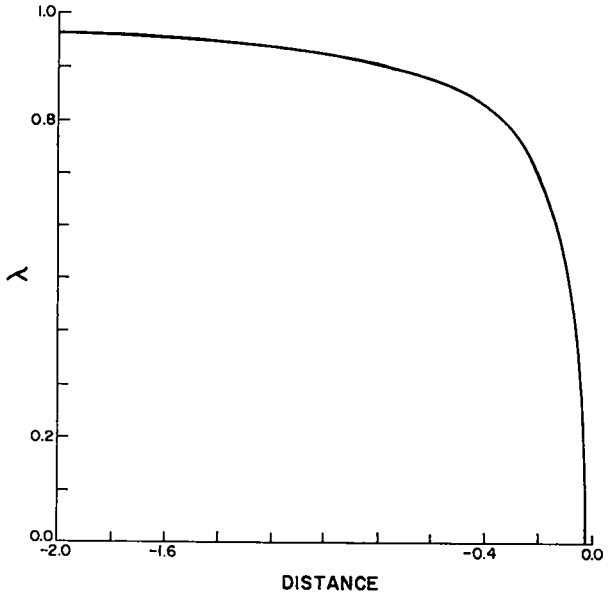

Fig. 41. Reaction extent λ vs distance.

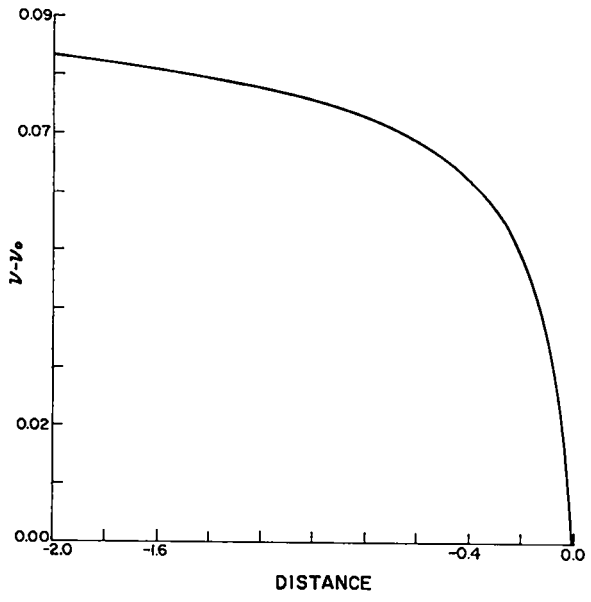

Fig. 42. Reduced volume fraction $\nu-\nu_o$ vs distance.

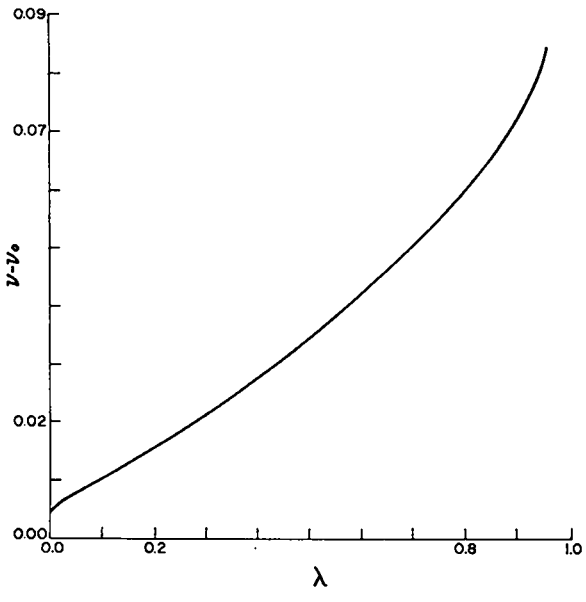

Fig. 43. Reduced volume fraction $\nu-\nu_o$ vs reaction extent λ.

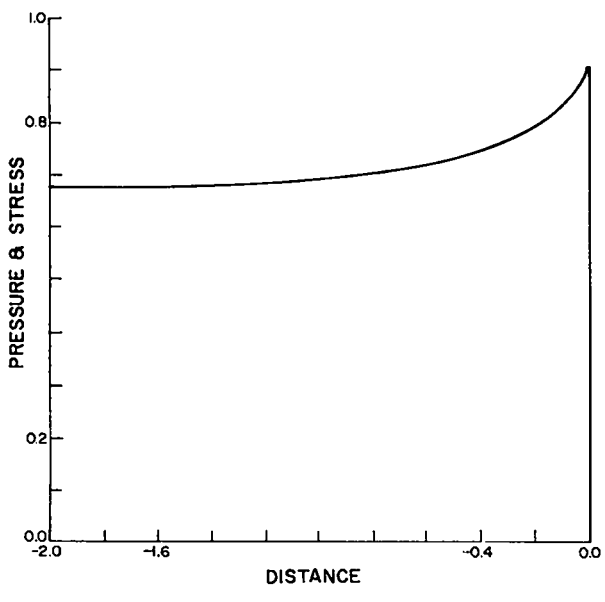

Fig. 44. Pressure and stress vs distance.

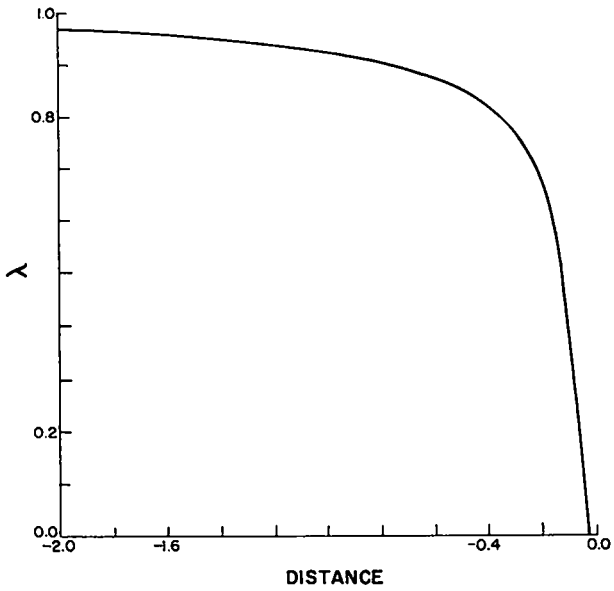

Fig. 45. Reaction extent λ vs distance.

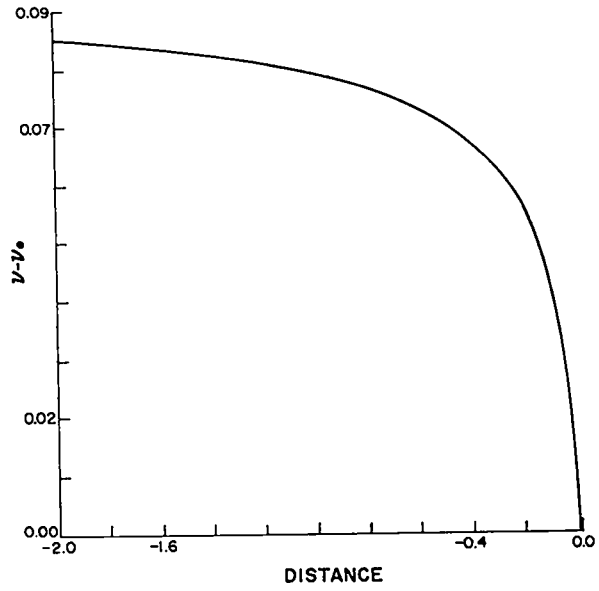

Fig. 46. Reduced volume fraction $\nu-\nu_o$ vs distance.

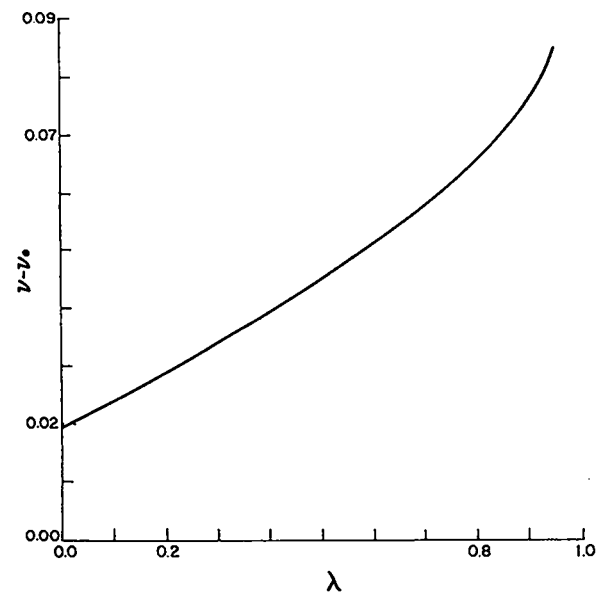

Fig. 47. Reduced volume fraction $\nu-\nu_o$ vs reaction extent λ.

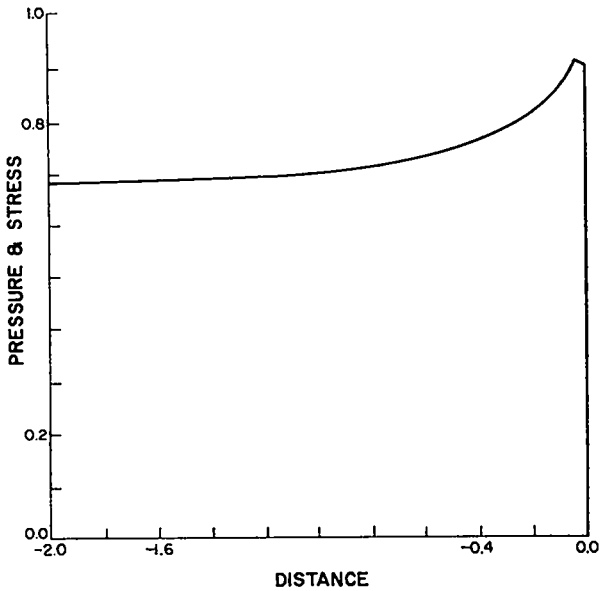

Fig. 48. Pressure and stress vs distance.

ACKNOWLEDGMENTS

I thank Jerry Wackerle and W. Fickett for several helpful discussions. In particular, the idea of eliminating the energy equation by choice of a simple equation of state is due to W. Fickett. An earlier problem, solved by W. Fickett, that motivated this work is found in Los Alamos Scientific Laboratory report LA-6739-MS (March 1977).

REFERENCES

1. Jerry Wackerle, R. L. Rabie, M. J. Ginsberg, and A. B. Anderson, "A Shock Initiation Study of PBX-9404," to be published in the Proceedings of the Symposium High Dynamic Pressure, Paris, France, August 28-30, 1978.

2. J. W. Nunziato, E. K. Walsh, and J. E. Kennedy, "A Continuum Model for Hot Spot Initiation of Granular Explosives," to be published in the Proceedings of the Symposium High Dynamic Pressure, Paris, France, August 28-30, 1978.

3. J. von Neumann, "Theory of Detonation Waves," Office of Scientific Research and Development Section B-1, OSRD 549 (May 4, 1942).

4. W. Herrmann, "Constitutive Equation for the Dynamic Compaction of Porous Materials," J. Appl. Phys. 40, 2490-2499 (1969).

5. S. C. Cowin, "Thermodynamic Model for Porous Materials with Vacuous Pores," J. Appl. Phys. 43, 2495-2497 (1972).

6. Michael Carrol and Albert C. Holt, "Suggested Modification of the P-α Model for Porous Materials," J. Appl. Phys. 43, 759-761 (1972).

7. E. Jouguet, Mécaniques des explosifs (O. Doin et Fils, Paris, 1917).

8. W. Fickett and W. C. Davis, "Steady Detonation," in Detonation (University of California Press, 1979).

9. L. D. Landau and E. M. Lifshitz, "Viscous Fluids," in Fluid Mechanics, J. B. Sykes and W. H. Reed, Trans. (Pergamon Press, New York, 1975), Chap. 2, pp. 47-49.

APPENDIX

A DISCUSSION OF THE EIGENVALUE PROBLEM

Discussion in the text shows that the reaction path $\lambda = \lambda(v)$ can be calculated for the system independently of the current thermodynamic state. The relation $\lambda = \lambda(v)$ holds along the Rayleigh Line, which is a straight line (inviscid flow) in the p-v plane of slope $(\rho_o D)^2$. The entire flow problem is reduced to a

matter of numbers by requiring the Rayleigh Line to be tangent to some equation-of-state locus at some point in the p-v plane. This appendix gives the reasoning that leads to a solution of the tangency problem.

Recall that the function

$$p_r = \lambda q_1 + (\nu - \nu_o)\, q_2 \qquad \text{(A-1)}$$

gives the reaction pressure. To see how this function behaves, it is worth noting that for any path $\lambda = \lambda(\nu)$, in which λ is a monotonic increasing function of ν, the function p_r has as its largest possible value q_1 and as its smallest possible value $(1-\nu_o)q_2$. p_r at $\lambda = 1$, $\nu = 1$ (the end of the reaction zone) is $q_1 + (1-\nu_o)q_2$. These special points are shown in Fig. A-1.

Two cases between the extremes are also shown in Fig. A-1 as the solid lines. One of these has an extremum that is a maximum, the other, one that is a minimum, of p_r. One can get a path $\lambda = \lambda(\nu)$ that has both a maximum and a minimum of p_r. If p_r has no maximum on the interior of the interval $0 < \lambda < 1$, the maximum value will be $p_r = q_1 + (1 - \nu_o)q_2$. This is less by $(1 - \nu_o)q_2$ than the corresponding case with $A = 1$.

In pressure-volume space, the fact that p_r has a maximum along the reaction path (and hence the Rayleigh Line) allows a complete solution. Given the maximum value of p_r along the Rayleigh Line, I construct a Rayleigh Line that is tangent to the curve (see Fig. A-2),

$$p = 1/2\ (\rho-\rho_o)^2 + p_r(\max) \quad .$$

A tangency condition must hold because the largest value of p_r on the Rayleigh Line is $p_r(\max)$. Note that the reaction zone ends in a point below the tangent point that has weak (supersonic) character. This is manifested as a plateau at a pressure $p - p_w$ that grows at a rate $d\ell/dt = D - (u + c)$ where u and c are particle velocity and local sound speed at the end of the reaction zone and ℓ is the length of the plateau.

This class of detonations in which a maximum of $p_r < q_1$ occurs is called eigenvalue detonations because the detonation velocity cannot be found by simply considering the state of the system at the end of the reaction zone.

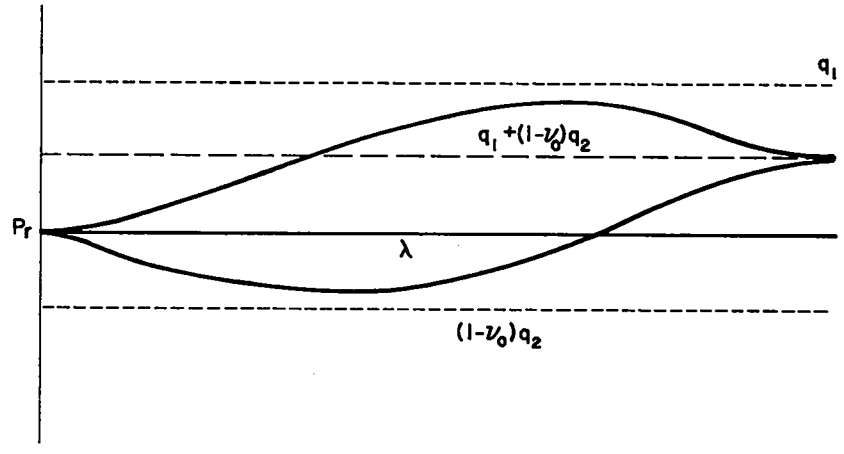

Fig. A-1. Upper and lower extremes for the function $p_r(\lambda)$ are shown as close dashed lines. The value of p_r at $\lambda = 1$ is shown as the long dashed line. The solid curves are possible p_r loci for various reaction paths.

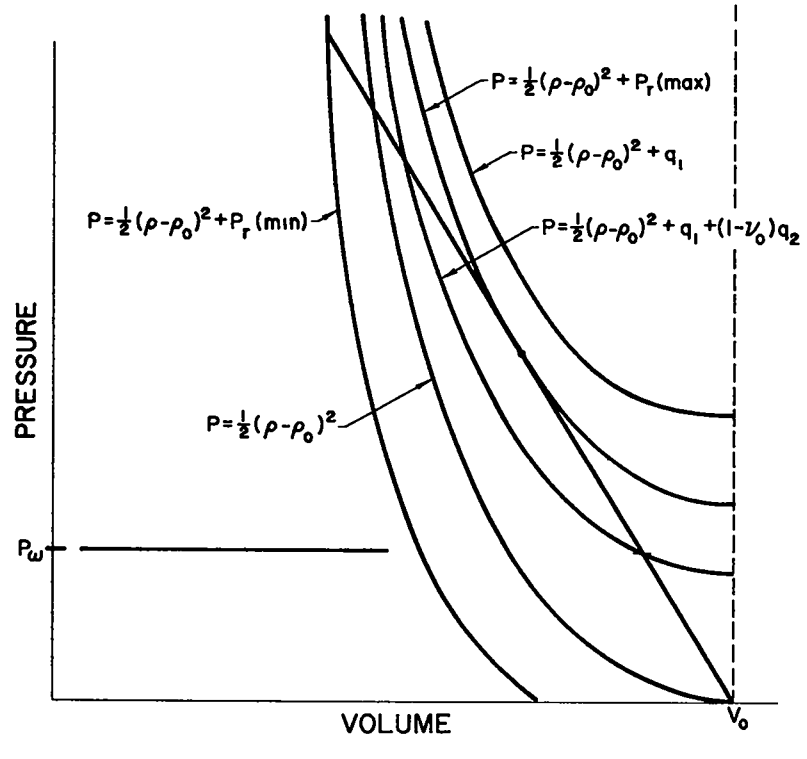

Fig. A-2. A pressure-volume plane representation of an eigenvalue detonation in the porous-reactive analog.

☆U.S. Government Printing Office: 1979 – 677-013/188

Printed in the United States of America. Available from
National Technical Information Service
US Department of Commerce
5285 Port Royal Road
Springfield, VA 22161

Microfiche $3.00

001-025	4.00	126-150	7.25	251-275	10.75	376-400	13.00	501-525	15.25
026-050	4.50	151-175	8.00	276-300	11.00	401-425	13.25	526-550	15.50
051-075	5.25	176-200	9.00	301-325	11.75	426-450	14.00	551-575	16.25
076-100	6.00	201-225	9.25	326-350	12.00	451-475	14.50	576-600	16.50
101-125	6.50	226-250	9.50	351-375	12.50	476-500	15.00	601-up	

Note: Add $2.50 for each additional 100-page increment from 601 pages up.